GRID 2025

Institute of Mathematical Problems of Biology

Russian Academy of Sciences

DNA Based Quantum Bioinformatics

V.D. LAKHNO

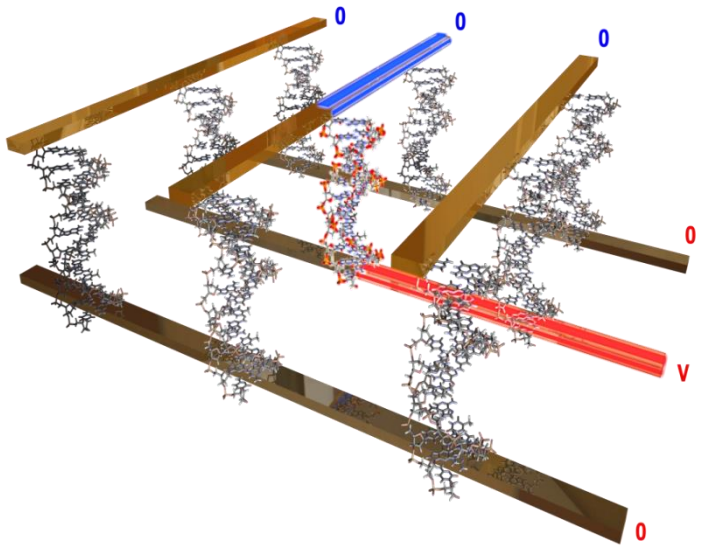

INFORMATICS

Informatics is the study of computational systems, especially those for data storage and retrieval.

synonymous – computer science, information science, information science, information technologies etc.

(Wikipedia)

Bioinformatics

Bioinformatics – is the field that develops methods and software tools for understanding biological data.

Includes:

- Sequence analysis
- Gene and protein expression
- Analysis of cellular organization
- Structural bioinformatics
- Databases

New direction:

Bioinformatics as informatics on the basis of biocomputer technologies and DNA information storages and nanobioelectronics.

DNA based information technologies. Nanobioelectronics

General problem:

The amount of generated information grows with exponential rate.

Cumulative information volume generated by humanity is about several billion terabytes per year.

Contemporary state:

The density of information store by modern media (magnetic and optical devices: compact disks, hard discs, magnetic tapes) as usual does not exceed 1000 Gb/mm^2.

The low density of information storage leads to the problem storage capacity confinement

The possibility of data losing in length of time.

This request the development of new methods of information storage and handling.

Perspectives to solve the problem:

DNA – memory

DNA – calculations

DNA - computer

DNA is essential digital, L. Adelman

DNA – memory

Modern technology of DNA synthesis and sequenation opens the way to wright on DNA: setup of 64 kilobyte data which contains a book, 11 JPG pictures and Java SCRIPT program (2012), (Church G.M. et al, Science, 2012, v.337, p. 1628)

16 Gigabyte of Wikipedia (2019)

The density of DNA information density storage (billion terabyte) / gram – billion time greater then on modern media (K.Matange, Nature Communications, (2021)12:1358)

Disadvantages

The rate of information placement on DNA (e.g. the memory) can not compete with modern media. Nevertheless DNA has advantage information density and costs of storage.

(The price of coding: 1000 $ / megabyte, reading 100 $ / megabyte)

Mistakes arising in realization of DNA – memory fall, exchange, replacer, substitution, insets, tandem duplication

DNA - READING

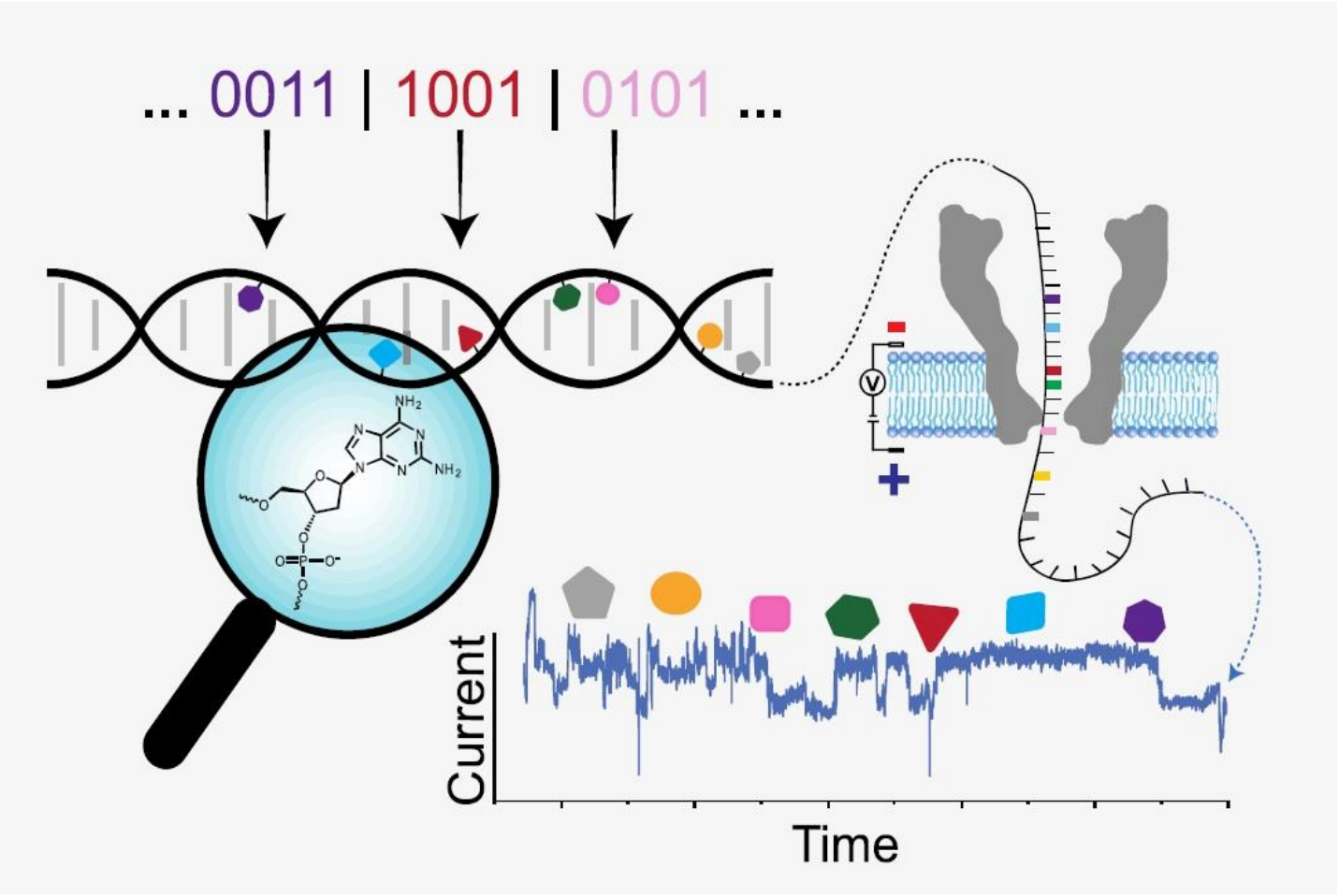

Expanding the Molecular Alphabet of DNA-Based Data Storage Systems with Neural Network Nanopore Readout Processing
S. Kasra Tabatabaei at al, Nano Lett. 2022, 22, 1905−1914

DNA – calculations, DNA – computer

(DNA – cryptography, DNA – stenography)

DNA – computer – calculations proceed using chemical reactions between DNA fragments

Advantages

Polynomial time for solving combinatorial problems is achieved due to parallelism of calculations (a lot of semiltaneouns chemical reactions)

Disadvantages

Voyageur problem – optimal path for graph with 7 nodes (Adelman 1994)

The problem with 200 nodes needs the mass of DNA which exceeds the earth mass

Potential application of DNA in nanobioelectronics

DNA nanowires
DNA nanobiochips
DNA nanomotors
DNA posistors
DNA tunneling diods
DNA transistors
DNA biosensors
DNA quantum computers

V.D. Lakhno, DNA Nanobioelectronics, Int. J. Quant. Chem., 2008;
V.Lakhno, A.Vinnikov, Molecular devices based on DNA, MBB 2021

Charge transfer in oligonucleotides

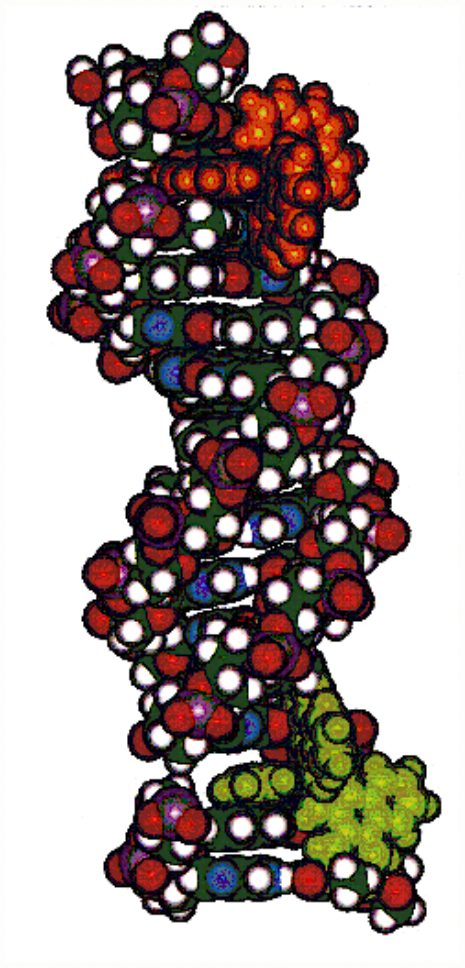

Ruthenium – rhodium molecular complexes are used as donors and acceptors in experiments on electron transfer in DNA.

The donor and the acceptor are linked by a covalent bond to a DNA fragment containing 15 nucleotide pairs.

Nanotransistor

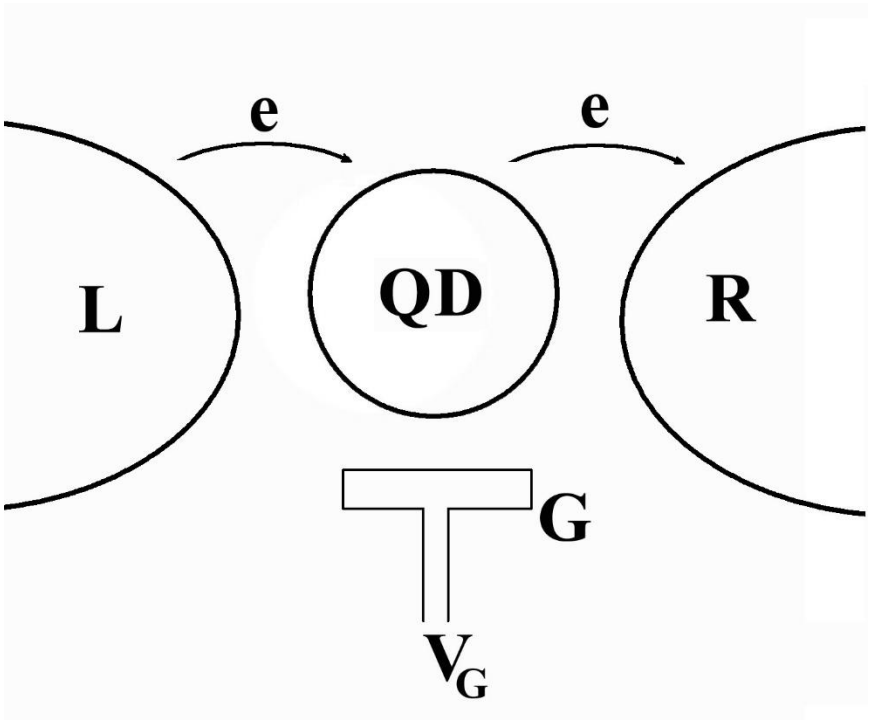

The nanotransistor scheme is shown consisting of quantum dot (QD) connected to electrodes L and R.

G – denotes the gate electrod cannected to the potential $V_{G.}$

DNA FIELD TRANSISTOR

source **drain**

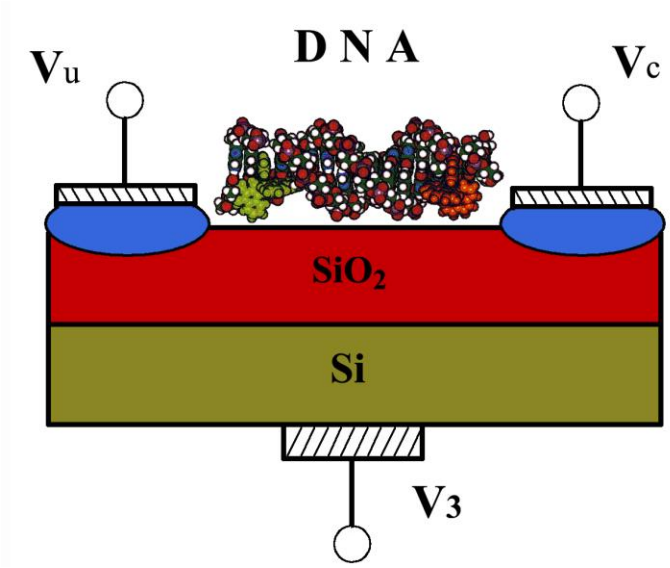

gate

K.-H.Yoo, D.H.Ha, et al, Phys.Rev.Lett., 2001, 87, 198102

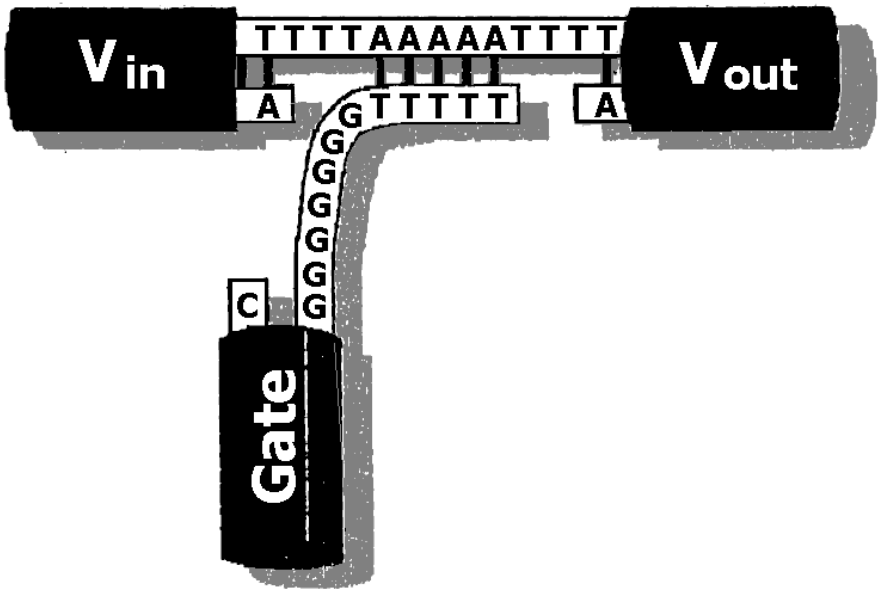

E. Ben-Jacob et al, patent, 2007

DNA nanotechnologies

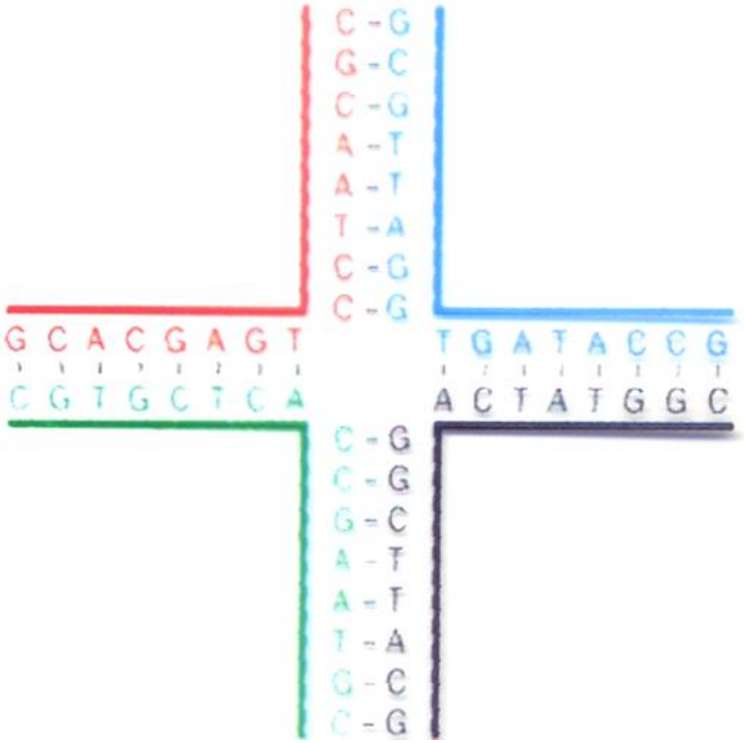

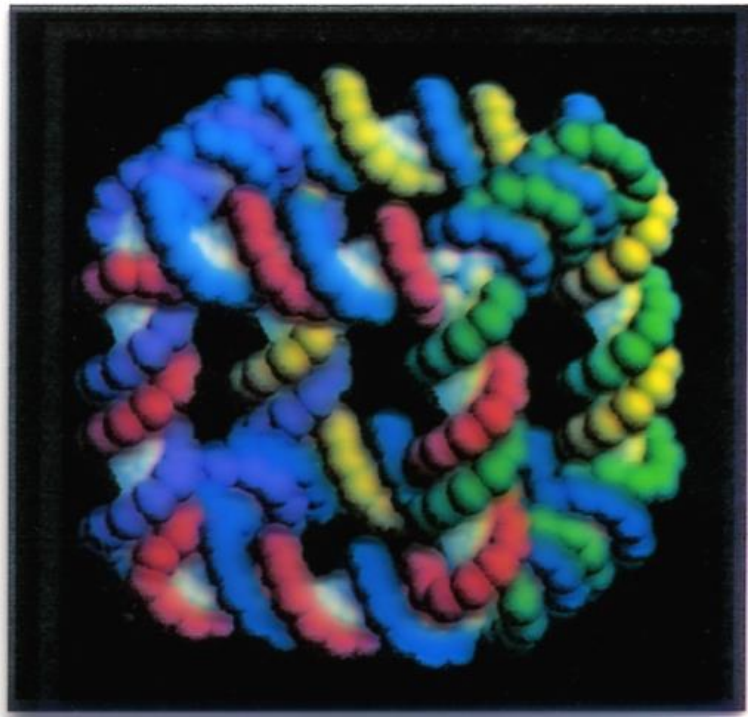

The properties of DNA selfconstruction can be used for design of different structures

(C.Dekker at al., Physics World, 2001)

Dip - Pen Nanolithography

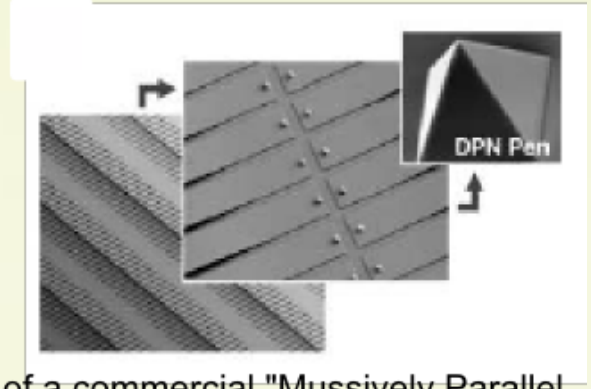

Sem images of a commercial "Mussively Parallel Pen" array (A.Mirkin et al Angew.Chem.Int.,2004)

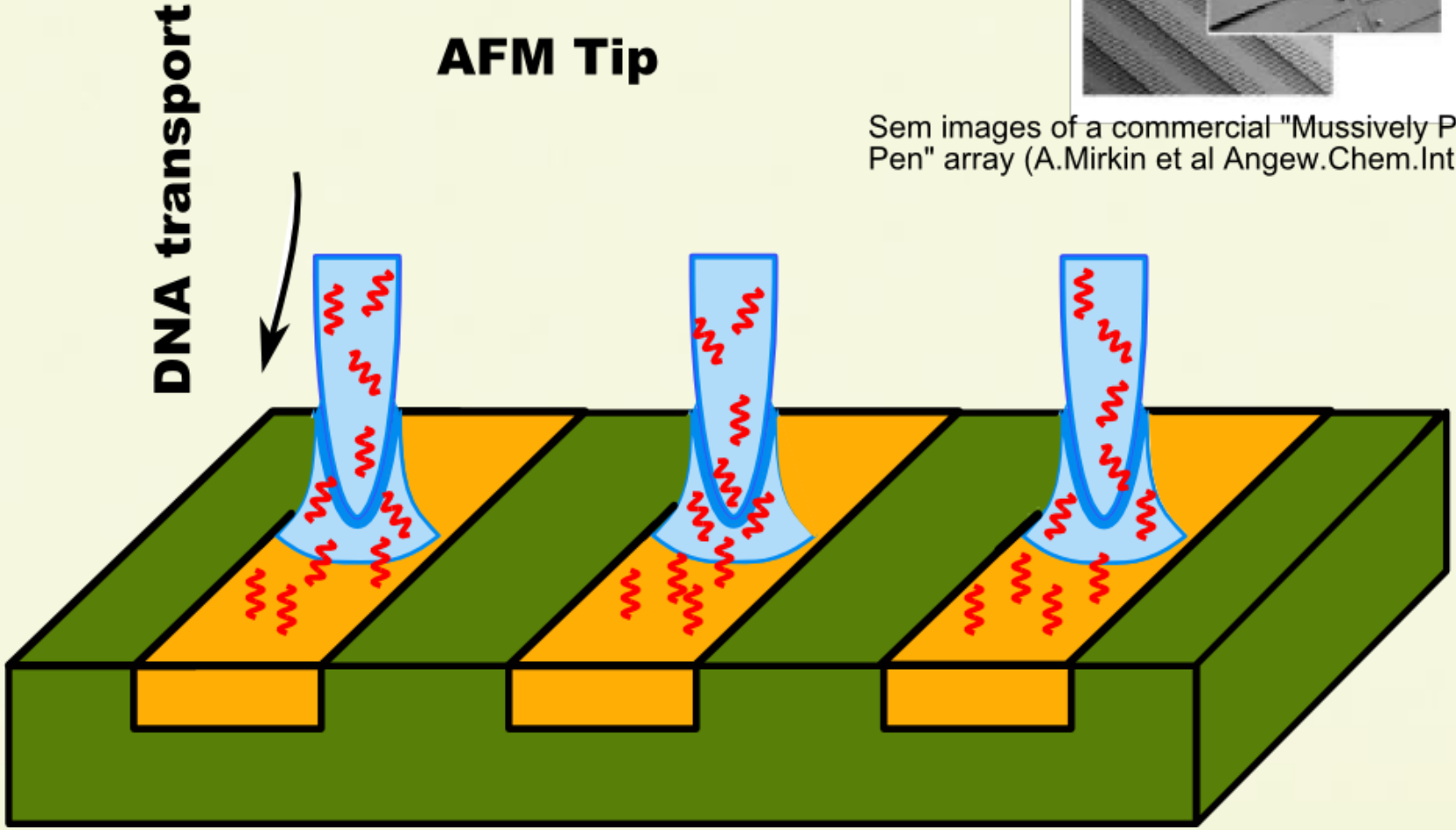

Single-Molecule Conductance Measurements of Single- and Double-Stranded DNA Oligonucleotides

ChemPhysChem v.7 n.1 pp.94-98

H. van Zalinge*, D.J. Schiffrin*, A.D. Bates[+], W. Haiss*, J. Ulstrup[#],

R.J. Nichols*

* Centre for Nanoscale Science, Chemistry Department, University of Liverpool, Unated Kingdom

[+] School of Biological Science, University of Liverpool, Unated Kingdom

[#] Department of Chemistry, Technical University of Denmark

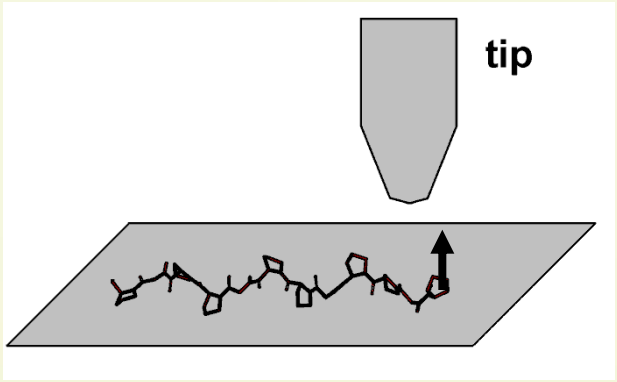

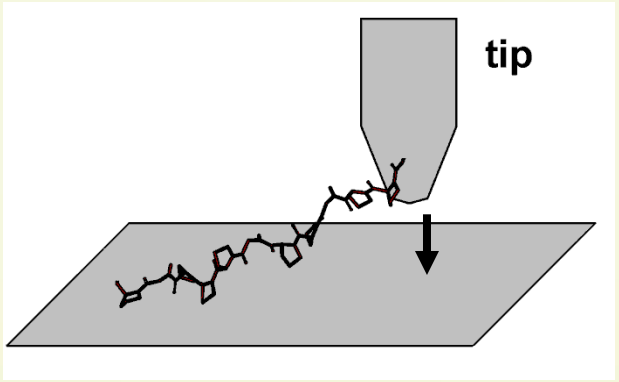

Hole injection into DNA

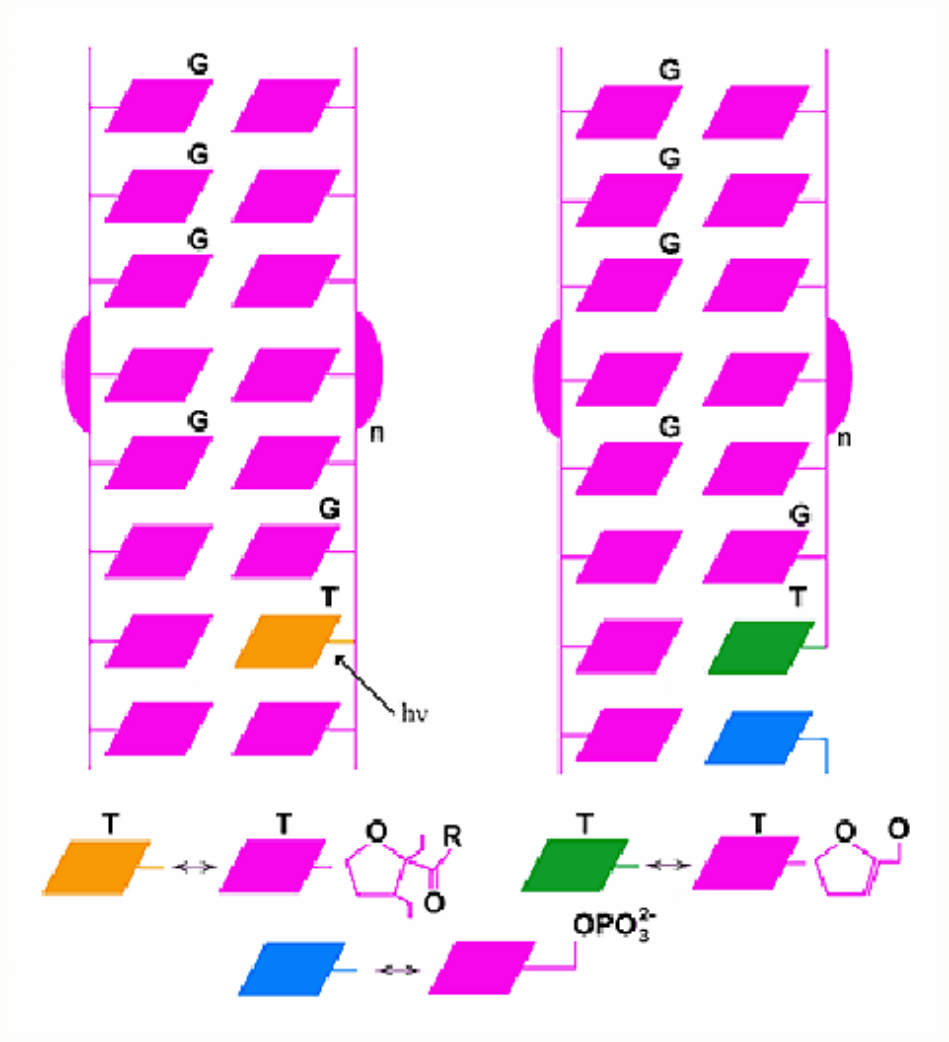

(Giese et al experiments)

Electrical transport through DNA molecules. Direct measurement.

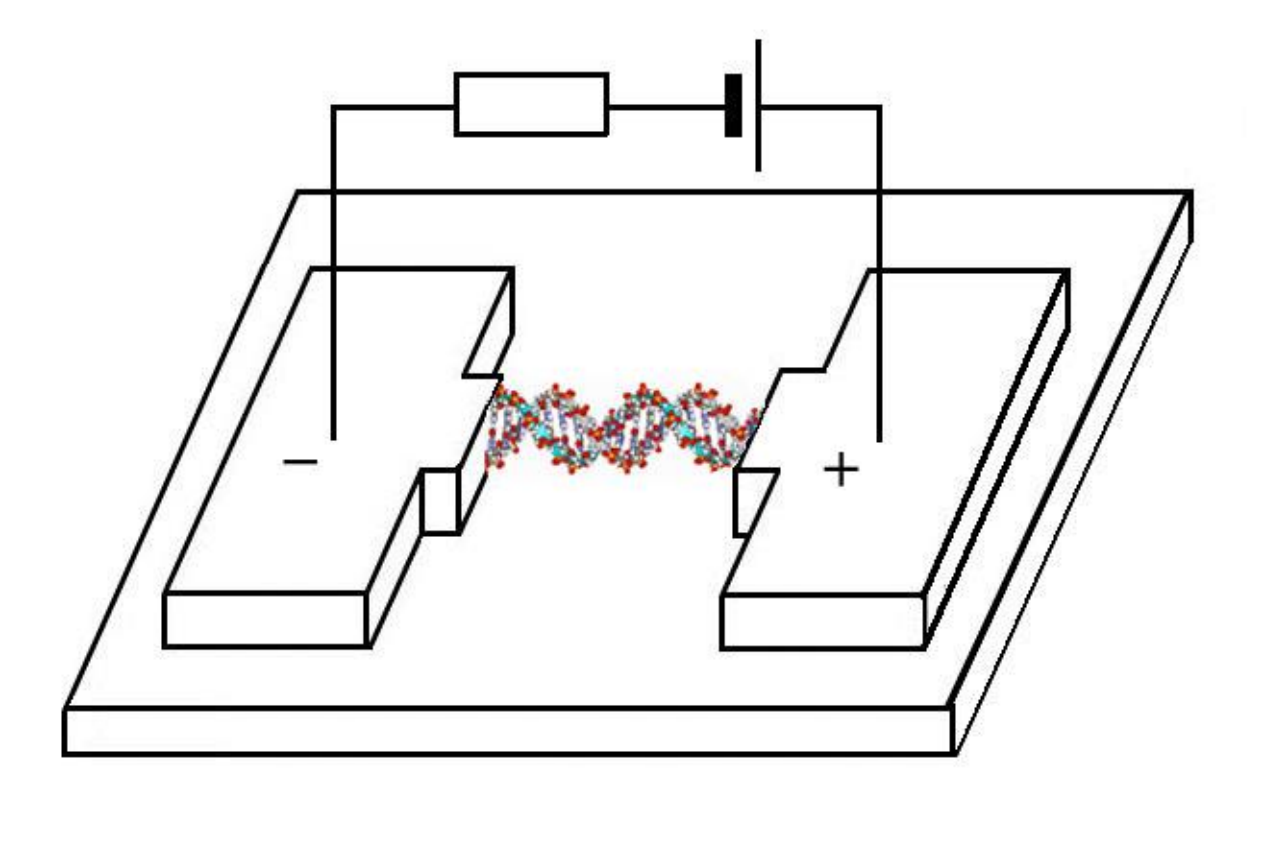

D.Porath et al, Nature, **403**, (2000), 635

Basic linear biopolymer - DNA

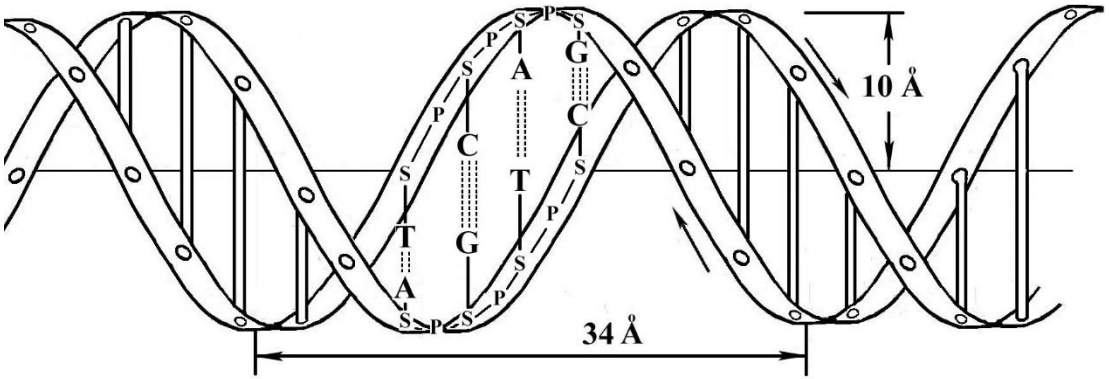

Space DNA structure

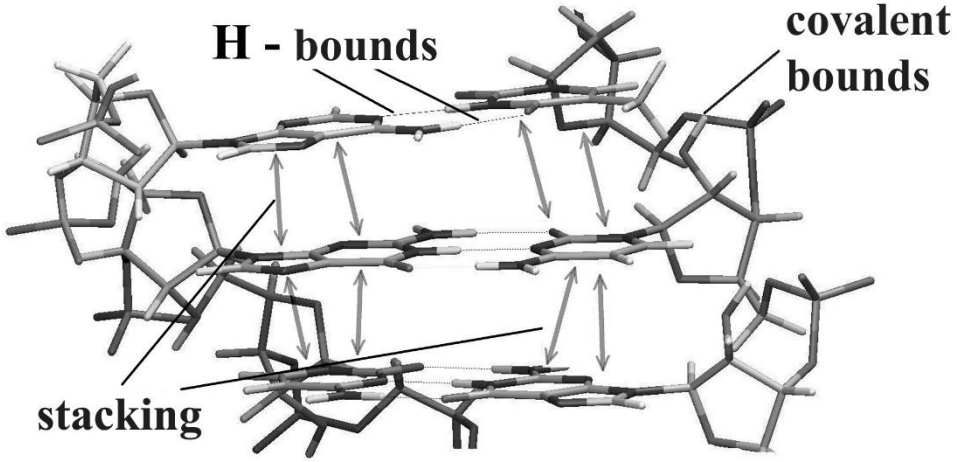

Relative space positions of H – bounds and stacking interactions in DNA

Mechanical DNA models

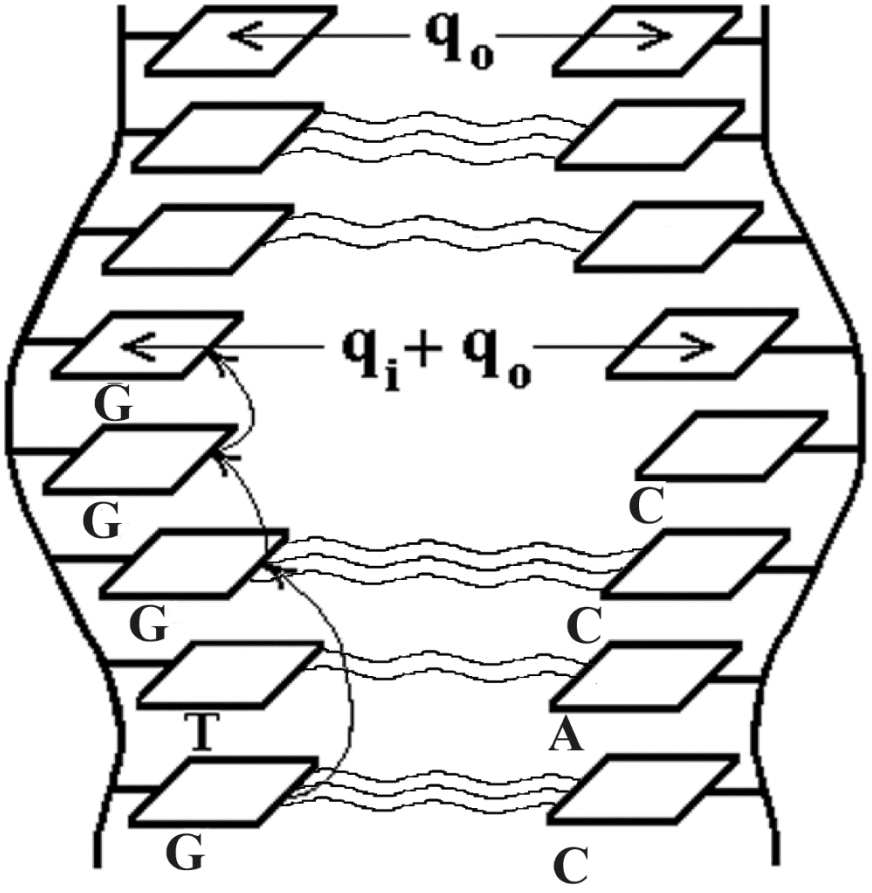

Covalent bound ~ 3,6 eV
Stacking interaction ~ 0,14 ÷ 0,63 eV
H-bound ~ 0,13 ÷ 0,26 eV

DNA Thermodynamics

$$H = \sum_{n=1}^{N} \frac{M}{2} \dot{y}_n^2 + \sum_{n=1}^{N} \{D_n (e^{-\alpha y_n} - 1)^2\} + \sum_{n=1}^{N-1} \left\{ \frac{k}{2} \left(1 + \rho e^{-\beta (y_n + y_{n+1})}\right) (y_n - y_{n-1})^2 \right\}$$

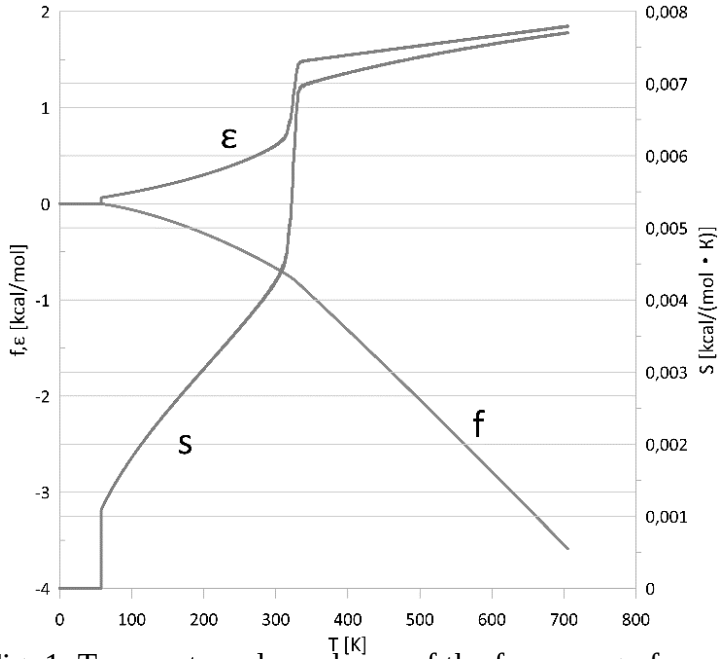

Fig. 1. Temperature dependence of the free energy f, energy ε and entropy s per a Watson-Crick pair for an AT chain of 100 base pairs.

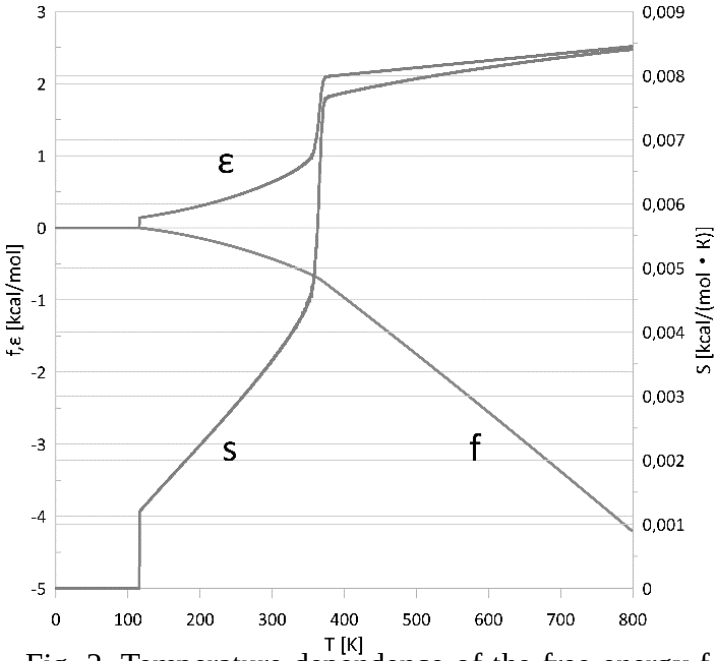

Fig. 2. Temperature dependence of the free energy f, energy ε and entropy s per a Watson-Crick pair for a GC chain of 100 base pairs.

I.Likhachev, A.Shigaev, V.Lakhno Phys.Lett.A 2024

"Kroemer's Lemma of Proven Ignorance"

If, in discussing a semiconductor problem, you cannot draw an Energy Band Diagram, this shows that you don't know what you are talking about, with the corollary.

If you can draw one, but don't, then your audience won't know what you are talking about.

"Quasi-electric fields and band offsets: teaching electrons new tricks".

Nobel Lecture, December 8, 2000, H. Kroemer.

Electron in a rigid chain

$$\hat{\mathrm{H}} = \sum_{n,m} \nu_{n,m} |n\rangle\langle m|$$

Homogeneous chain in the nearest neighbor approximation

$$\left(\nu_{n,n\pm1} = \nu,\ \nu_{n,m} = 0 \quad m \neq n \pm 1\right): \qquad |\Psi\rangle = \sum_n b_n |n\rangle$$

Schroedinger equation:

$$i\dot{b}_n = \nu\left(b_{n+1} + b_{n-1}\right) \qquad b_n(t) = e^{-iW_k T} R_{n,k}, \quad R_{n,k} = \frac{e^{ikn}}{\sqrt{N+1}}$$

For Poly G/Poly C chain:

$$W_k = 2\nu\cos k, \quad k = \pm\frac{2\pi l}{N}, \quad l = 0,1,2,\ldots\frac{N}{2}$$

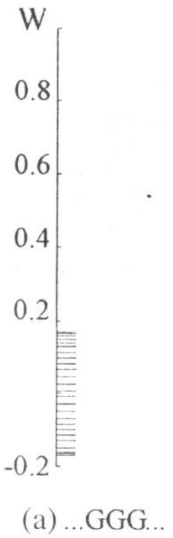

$\Delta W = 4\nu$ - **conductivity band width.**

Regular chains

Band structure for Poly(GT)/Poly(CA)

$$n = 2j: \quad \nu_{2j,2j} = 0, \quad \nu_{2j,2j+1} = \nu_1, \quad j = 0, \pm 1, \pm 2, \cdots$$

$$n = 2j+1: \quad \nu_{2j+1,2j+1} = \alpha_T, \quad \nu_{2j,2j-1} = \nu_2$$

Eigen value equations:

$$W_k R_{2j,k} = \nu_1 R_{2j+1,k} + \nu_2 R_{2j-1,k}$$

$$W_k R_{2j+1,k} = \alpha_T R_{2j+1,k} + \nu_2 R_{2j+2,k} + \nu_1 R_{2j,k}$$

$$R_{2j+1,k} = u_2 \exp\left[ik(2j+1)\right], \quad R_{2j,k} = u_1 \exp\left[ik(2j)\right],$$

$$W_k^{\pm} = \frac{\alpha_T}{2} \pm \sqrt{\left(\alpha_T / 2\right)^2 + \left(\nu_1^2 + \nu_2^2 + 2\nu_1\nu_2 \cos 2k\right)^2}$$

Poly(GT)/Poly(CA)

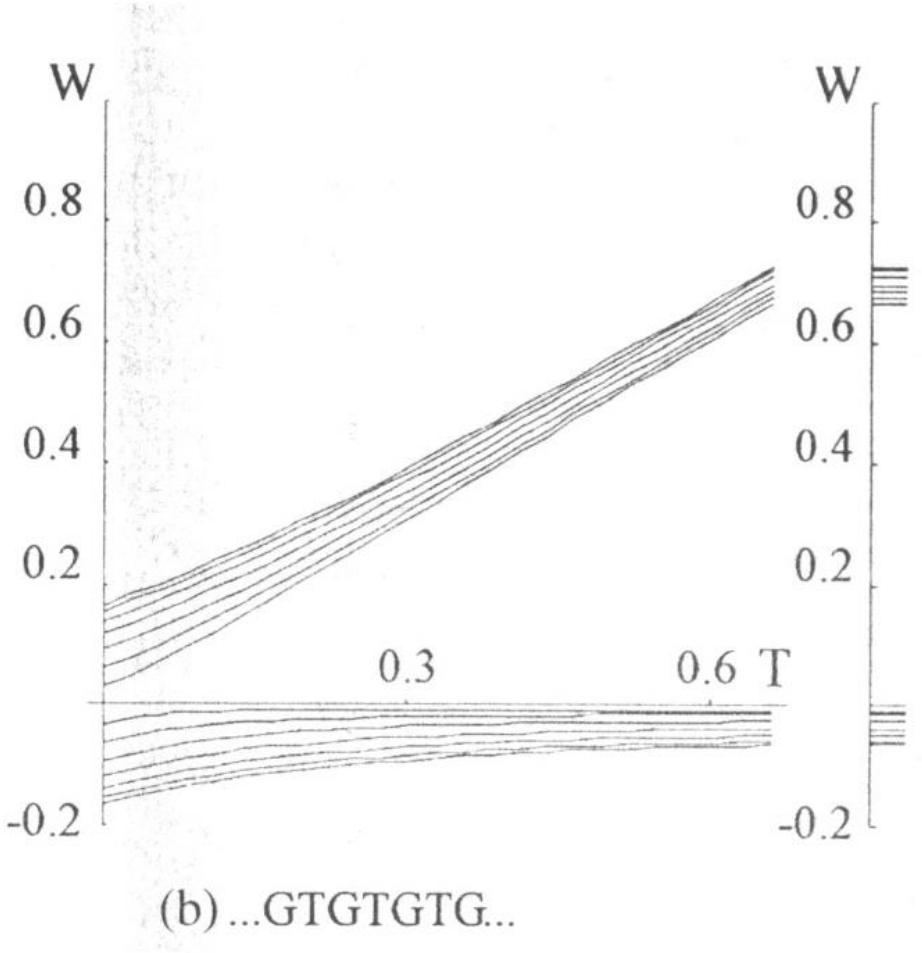

Band structures of various regular chains

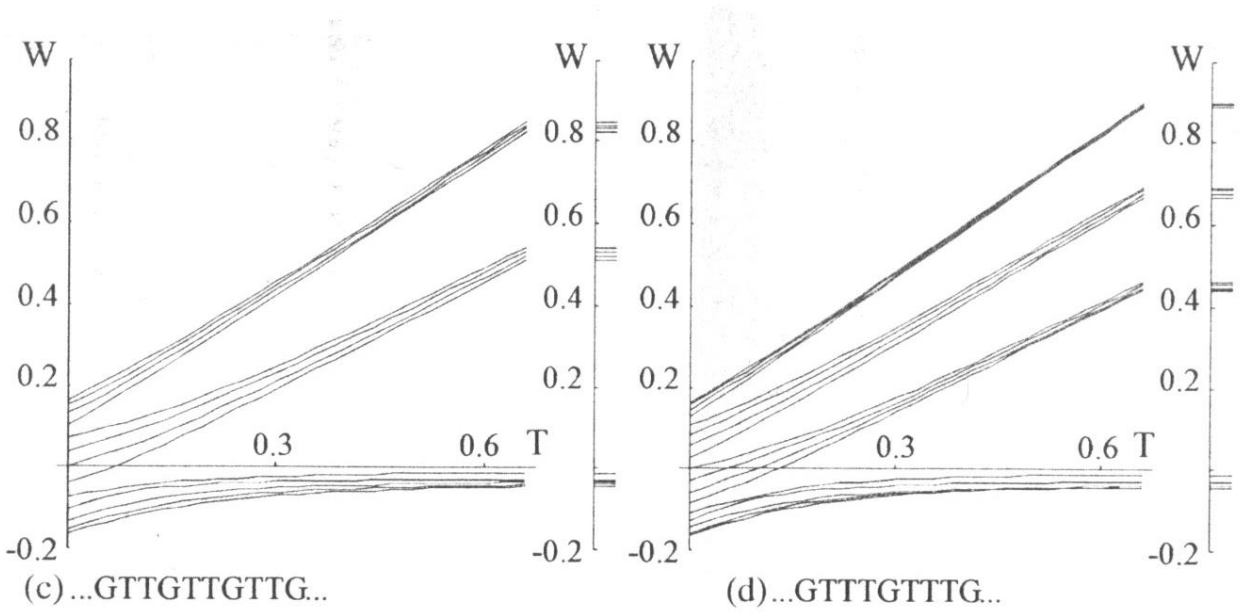

For regular chains, that contain **m** sites in an elementary cell, there are **m** different branches determining their band structure.

V.D.Lakhno in "Modern Methods for Theoretical Physical Chemistry of Biopolymers", Ed. By E.B.Staricov , J.P.Lewis, S.Tanaka, (2006), Elsevier

V.D.Lakhno, V.B.Sultanov, Theor.Math.Phys., v.176, 1194, (2013)

Conclusion

1. For regular chains, that contain m sites in an elementary cell, there are m different branches determining their band structure.

2. For finite regular chains the discrete levels can arise in the forbidden bands, which correspond to localised at the chain ends states (Tamm levels).

Formation of a soliton (polaron) state in a deformable chain

$$\hat{H} = \nu \sum_n \left(a_n^+ a_{n-1} + a_n^+ a_{n+1} \right) + \sum_n \alpha\, q_n\, a_n^+ a_n + \sum \frac{\hat{P}_n^2}{2M} + \sum \frac{k\, q_n^2}{2}$$

- Holstein model

$$\left| \Psi(t) \right\rangle = \sum_n b_n(t) a_n^+ \exp\left\{ -\tfrac{i}{\hbar} \sum_j \left[\beta_i(t) \hat{P}_j - \pi_j(t) q_j \right] \right\} \left| 0 \right\rangle$$

$$\left\langle \Psi(t) \left| q_n \right| \Psi(t) \right\rangle = \beta_n(t), \quad \left\langle \Psi(t) \left| \hat{P}_n \right| \Psi(t) \right\rangle = \pi_n(t)$$

Motion equation:

$$i\hbar \dot{b}_n = \alpha \beta_n b_n + \nu \left(b_{n-1} + b_{n+1} \right)$$

$$M \ddot{\beta}_n = -\gamma \dot{\beta}_n - k \beta_n - \alpha \left| b_n \right|^2$$

Exact solution for a rigid chain $(\alpha = 0)$

$$b_n(t) = \sum_m b_m(0) (-i)^{n-m} J_{n-m}\left(2\nu t / \hbar \right)$$

J_n **- Bessel function of the first kind, describes dynamics of the wavepackage spreading .**

Numerical solution for $(\alpha \neq 0)$

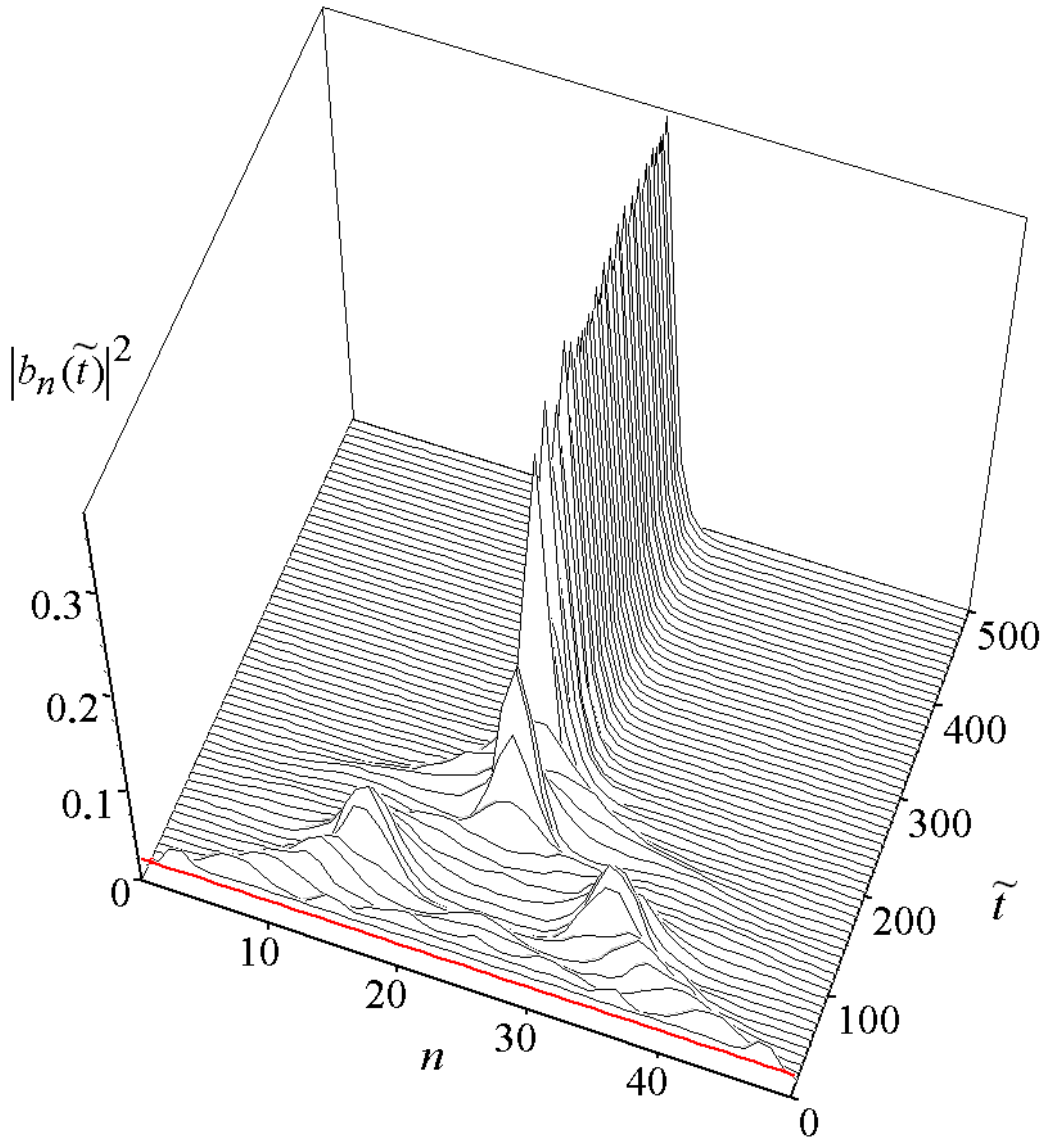

Formation of a soliton state

Formation of multisoliton states

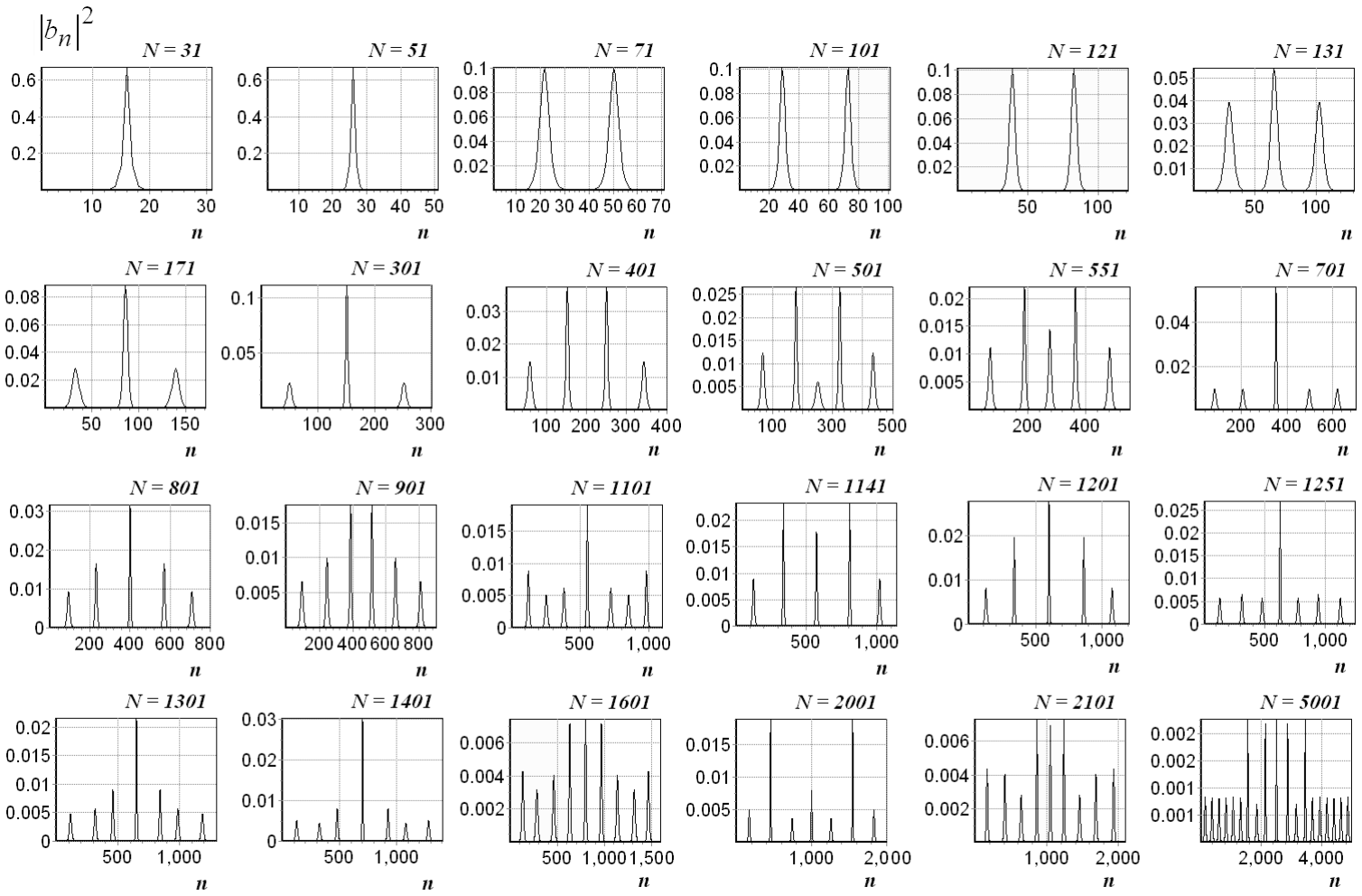

Lakhno V.D., Korshunova A.N., Mathem. Biol. And Bioinform., v.5, (2010), p.1-29.

Results of modelling

1) A delocalized state in the chain is unstable.
2) A polaron (soliton) state is formed both in the presence and in the absence of dissipation.
3) The time for which a localized state is formed depends greatly on the wave function phase.
4) In multisoliton states objects with fractional electron charge are formed which can be found experimentally.

Electron motion in an electric field in a rigid chain $(\alpha = 0)$

Exact solution of Schroedinger equation for a rigid chain:

$$b_n(t) = \sum_{m=-\infty} b_m(0)(-i)^{n-m} e^{-i(n+m)\omega_\beta t} J_{n-m}(\zeta(t))$$

$$\zeta(t) = \frac{4\nu}{\hbar\omega_B} \sin\left(\frac{\omega_B t}{2}\right), \quad \hbar\omega_B = e\varepsilon a$$

$J_n(x)$ **- Bessel function of the first kind**

$$X(t) = \sum_n^N |b_n(t)|^2 na$$ **- displacement of the electron's mc**

$$X(t) = X(0) + \frac{2a\nu}{\hbar\omega_B}|S_0|(\cos\theta_0 - \cos(\omega_B t + \theta_0))$$

$$S_0 = \sum_{-\infty}^{\infty} b_m^*(0) b_{m-1}(0) = |S_0 e^{i\theta_0}|, \quad X(0) = a\sum_{-\infty}^{\infty} m|b_m(0)|^2$$

Oscillation amplitude $X(t) = 0$ **, if** $b_m(0) = 1$

Generation of Bloch oscillations in a deformable chain $(\alpha \neq 0)$

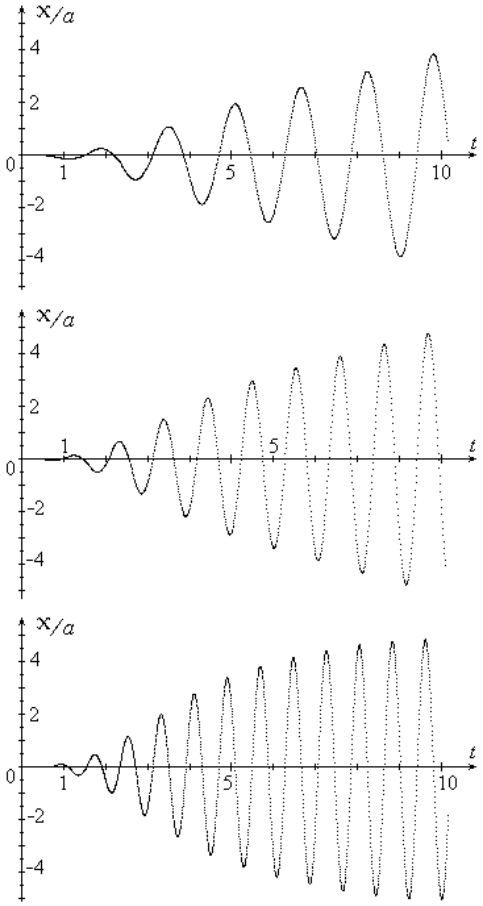

Time dependence of the hole's center of mass for various values of the electric field intensity (a) $\tilde{E} = 0.04$, (b) $\tilde{E} = 0.06$, (c) $\tilde{E} = 0.08$.

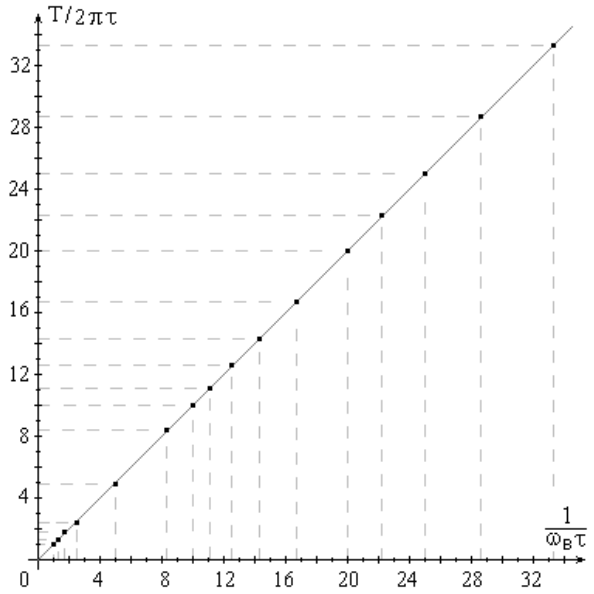

Solid line indicates the dependence of the Bloch oscillations period on the electric field intensity E ($T_B = 2\pi/\omega_B$ $\omega_B = eEa/\hbar$ - Bloch frequency), for $\kappa = 0$. Black dots indicate calculation values for $\kappa = 4$,

$\left(\alpha_n' \sim 1.3 \cdot 10^{-4} eV/\text{Å}\right)$

V.D.Lakhno, N.S.Fialko, Pis'ma v ZhETF, v.79, (2004), p.575-578.

Bloch oscillations in a homogeneous nucleotide chain

Conclusion

1) **It is shown that at zero temperature, a hole placed in homogeneous synthetic nucleotide chain with applied electric field demonstrates Bloch oscillations.**

2) **The oscillations of the hole placed initially on one of base pairs arise in response to disruption of the initial charge distribution caused by nucleotide vibrations**

3) **The finite temperature fluctuations result in degradation of coherent oscillations. The maximum permissible temperature for DNA "Bloch oscillator" occurrence is estimated.**

Soliton in a continuum approximation

$$i\hbar\frac{\partial b}{\partial t}+\frac{\hbar^2}{2m}\frac{\partial b}{\partial X^2}-\chi q b=0$$

$$\frac{\partial^2 q}{\partial t^2}+\Omega_0^2 q+\frac{\chi}{M}|b|^2=0$$

Davydov: how a soliton can move in the absence of dispersion (JETP, 1980)

$$q(\xi)=-\frac{\chi}{M\Omega_0^2}\int d\xi\,\omega(\xi'-\xi)|b(\xi')|^2,$$

$$\omega(\xi)=\frac{\theta(\xi)}{\sqrt{|\varepsilon|}}\sin\frac{\xi}{\sqrt{|\varepsilon|}},\quad \varepsilon=-\frac{V^2}{a^2\Omega_0^2},$$

$$b(\xi)=\frac{1}{\sqrt{2r}}\mathrm{ch}^{-1}(\xi/r),$$

$$r=4M(\hbar\Omega_0)_2/m\chi^2a^2,\quad \xi=(X-vt)/a,\quad q(\xi)=c\sin(\xi/\sqrt{|\varepsilon|})$$

V.D.Lakhno, Int. Quant. Chem.,V.110, (2010), pp.129-137

Emission of phonons by a moving soliton in a dispersionless chain.

Probability of charge's occurrence on site $|b_n|^2$

Displacements of sites u_n

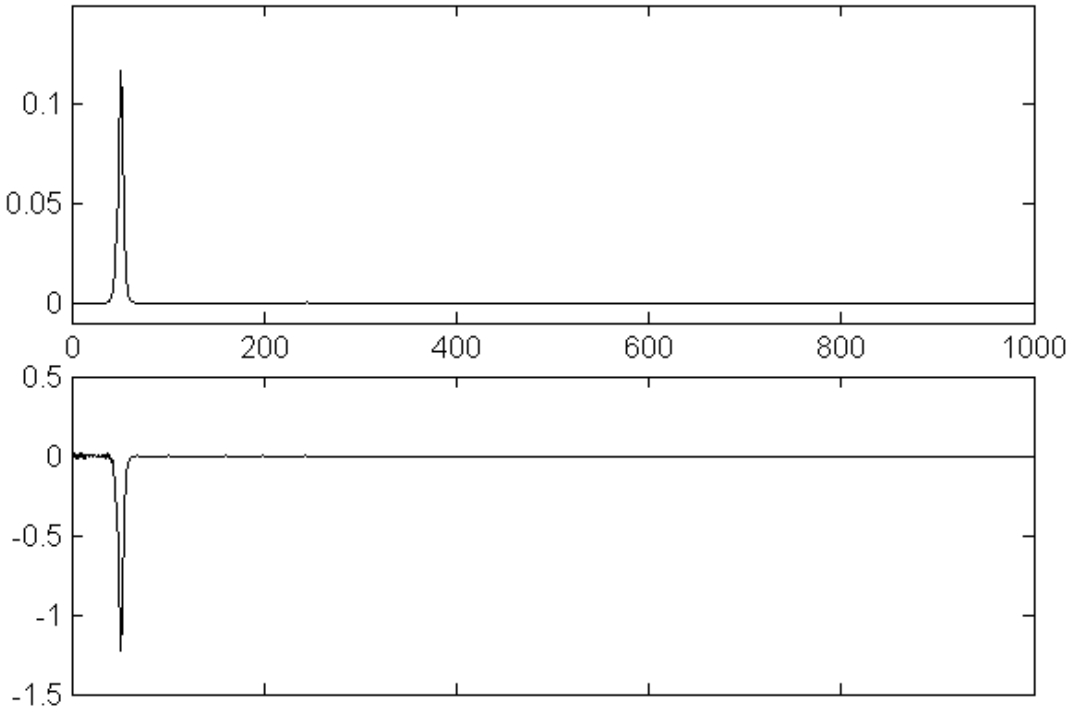

$$\eta = 0.1, \quad \omega^2 = 0.1, \quad \kappa = 0.1,$$

$$(\eta = \nu\tau/\hbar, \quad \omega = \Omega_0\tau, \quad \kappa = x^2\tau^3/M\hbar)$$

Dispersion

$\xi\left(q_{n-1}+q_{n+1}\right)$ - **for a discrete model**

$\xi\, a^2\, \frac{\partial^2 q}{\partial X^2}$ - **for a continuum model**

$\Omega^2 = \Omega_0^2 - \frac{2\xi}{M}\cos k$ - **discrete**

$\Omega^2 = \Omega_0^2 + V_0^2 k^2$ - **continuum**

Davydov:

for $V < V_0$ **- steady state of a soliton exists**

for $V > V_0$ **- steady state is impossible because of the emission**

Moving soliton

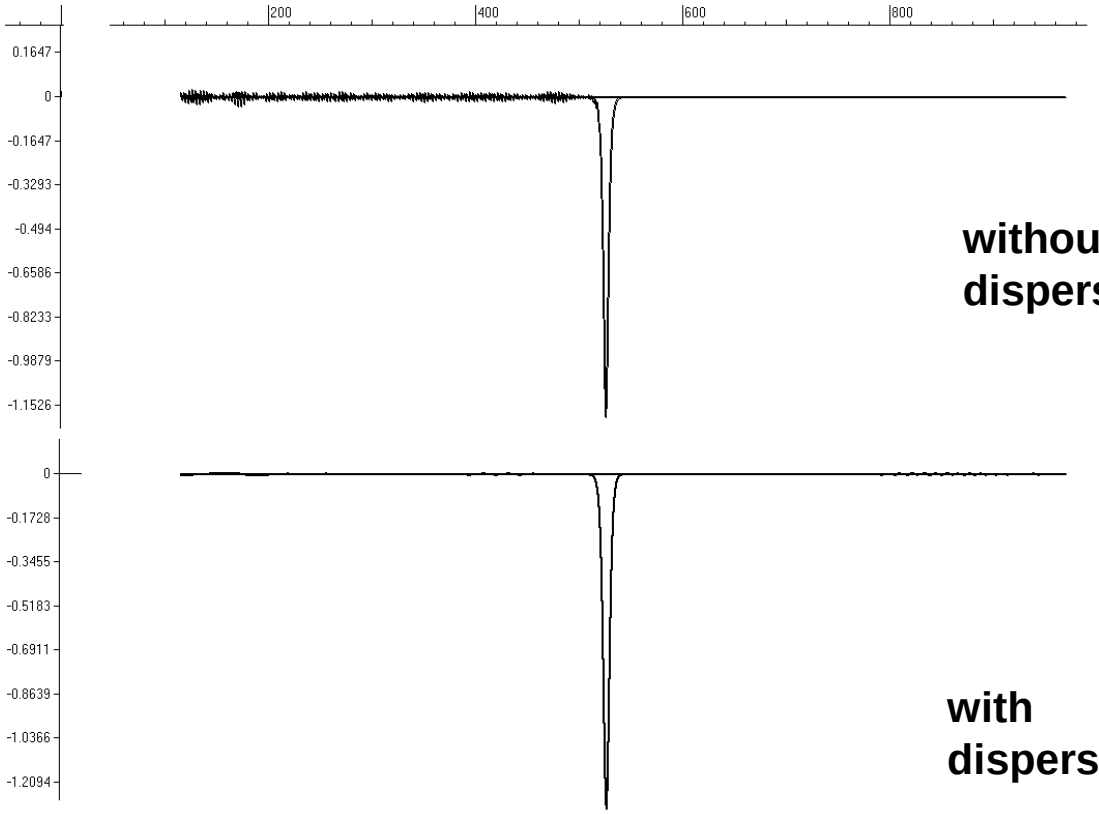

without dispersion

with dispersion

$$\eta = 0.1, \quad \omega^2 = 0.1, \quad \kappa = 0.1, \quad \xi = 0.001$$

Conclusion

1) In a molecular chain with dispersionless phonons at zero temperature the stationary motion is impossible.
2) In a molecular chain with disperionless phonons at zero temperature, a “quasistationary” moving soliton state of an excess electron is possible
3) As the soliton velocity vanishes, the path length of the excess electron exponentially tends to infinity.
4) In the presence of dispersion, when the soliton initial velocity exceeds the maximum group velocity of the chain, the soliton slows down until it reaches the maximum group velocity and then moves stationary at this maximum group velocity.

Homogeneous motion of a polaron over a chain in an electric field

$$i\hbar\dot{b}_n = \nu\left(b_{n-1} + b_{n+1}\right) + \alpha'\beta_n b_n + e\varepsilon a n b_n$$

$$M\ddot{\beta}_n = -k\beta_n - \alpha'\left|b_n\right|^2$$

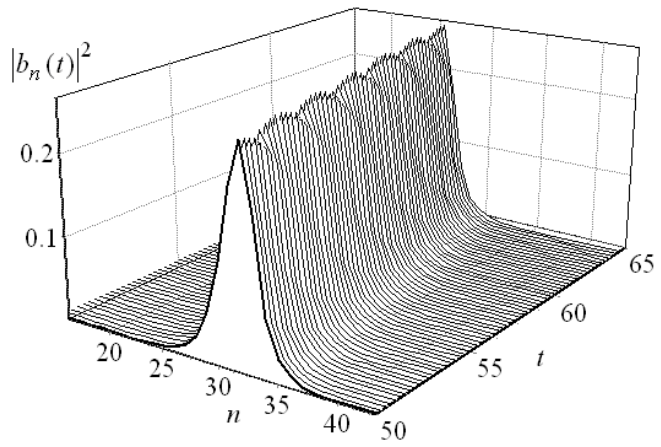

$E = 0.01, \quad \omega = 1, \quad \eta = 1.276, \quad \kappa = 2$

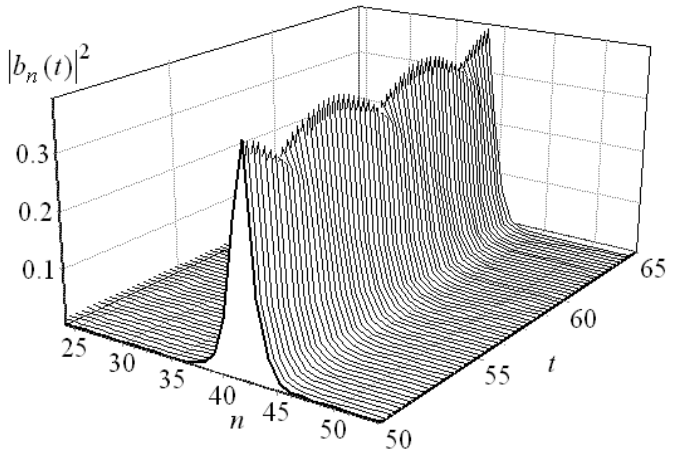

$\kappa = 3$

Peierls-Nabarro oscillations $\quad T_{PN} = 1/V, \quad V = dX/d\tilde{t}, \qquad X(\tilde{t}) = \sum_n n\left|b_n(\tilde{t})\right|^2$

Comparison of the theory with numerical experiments

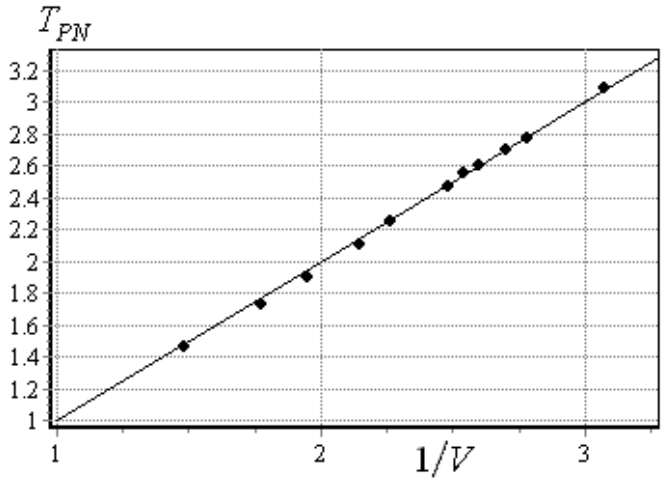

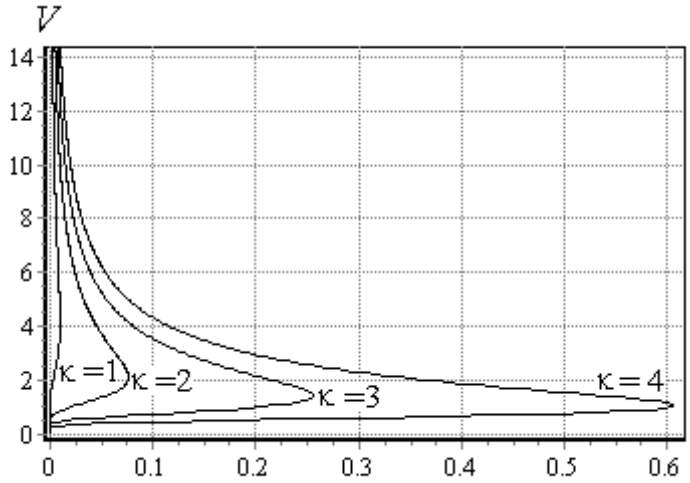

$$E = 2\pi^2 \frac{\omega^4 \eta^2}{\kappa} \frac{1}{V^4} \frac{1}{\sinh^2\left(2\pi\eta\omega/\kappa V\right)}$$

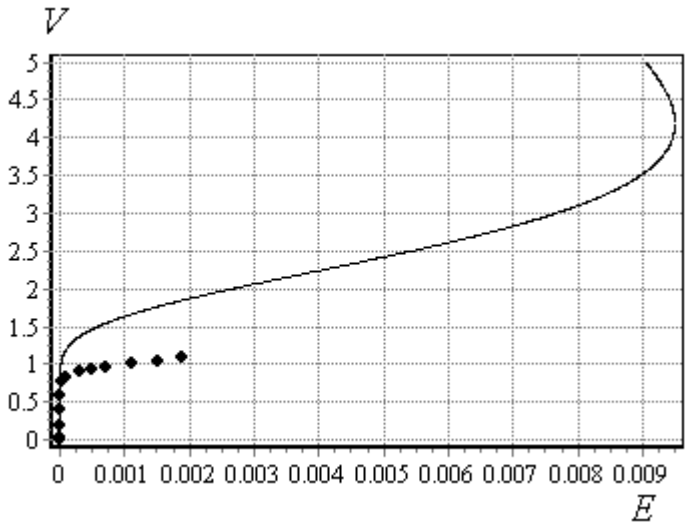

Lakhno V.D., Korshunova A.N., Eur. Phys. J. B, v.79, (2011), p.147-151.

Bloch oscillations in a constant electric field

$E = 0.1$

$\omega = 0.01,\ \omega' = 0.006$

$\eta = 1.276,\ \kappa = 1$

Poly A / *Poly* G (DNA chain)

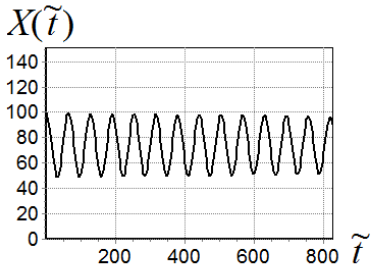

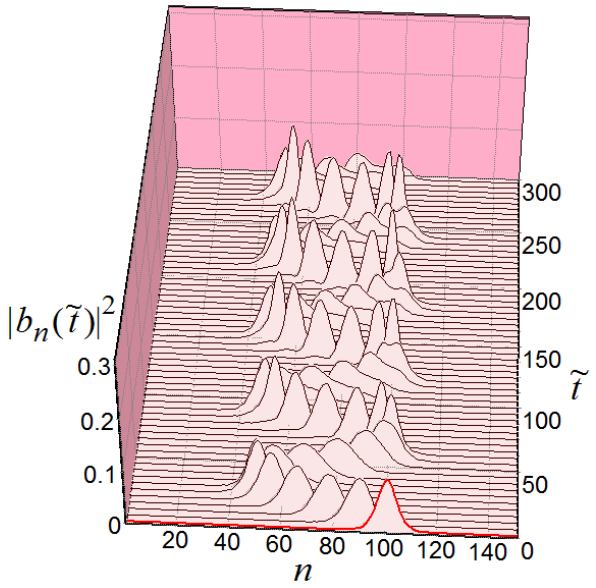

$X(\tilde{t}) = \sum_n |b_n(\tilde{t})|^2 n$ –

indicates the position
of the particle's center of mass

$E = 0.1$ corresponds to the
electric field intensity

$\mathcal{E} \approx 1.9 \cdot 10^5\, V/cm,\ \mathcal{E} = Eea/\hbar$

$E = 0.1$

$\omega = 1,\ \omega' = 1$

$\eta = 1.276,\ \kappa = 1$

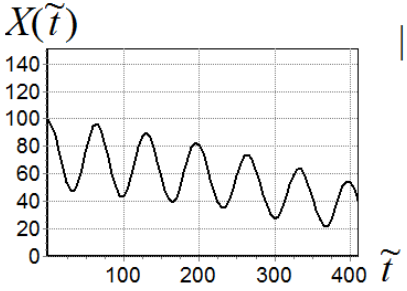

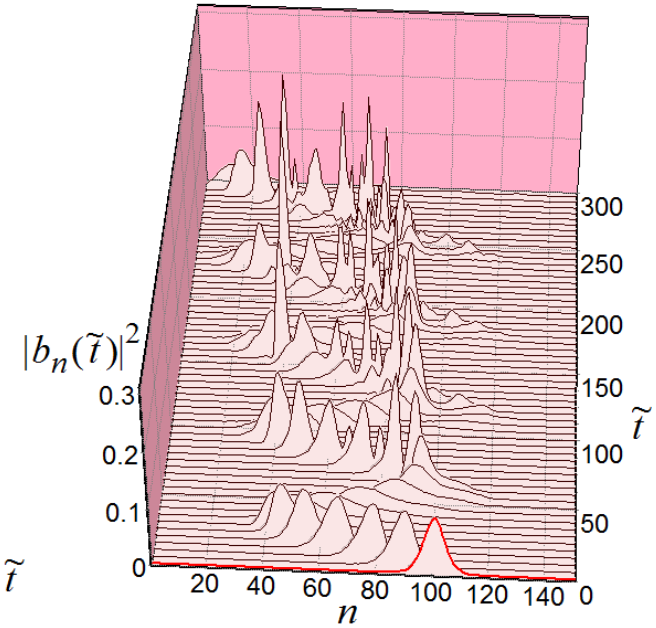

For the electric field of
intensity $E = 0.1$:

period of the Bloch oscillations

$$T_{BL} = \frac{2\pi}{E} \approx 62.8$$

the Bloch amplitude

$$Amp_{BL} = \frac{4\eta}{E} \approx 51$$

Conclusions

1) In a weak electric field a Holstein polaron moves uniformly experiencing small Peierls – Nabarro oscillation of its shape.
2) At critical value of the electric field intensity polaron starts oscillating at Bloch frequency, retaining its shape.
3) For sufficiently long time soliton becomes a breather that oscillates.
4) In all cases the polaron motion along the chain is infinite.

General approach to calculation of the mobility at high temperatures

Motion equations for Holstein Hamiltonian:

$$i\hbar \frac{db_n}{dt} = \alpha' q_n b_n + \nu\left(b_{b+1} + b_{n-1}\right)$$

$$M \frac{d^2 q_n}{dt^2} = -\gamma_f \frac{dq_n}{dt} - k\, q_n - \alpha' \left|b_n\right|^2 + A_n(t)$$

$$\left\langle A_n(t) \right\rangle = 0 \qquad \left\langle A_n(t) A_m\left(t + t'\right) \right\rangle = 2T\, \gamma_f \delta_{n\,m} \delta\left(t'\right)$$

$$\mu = \frac{e}{2T} \lim_{\varepsilon \to 0} \varepsilon^2 \int_0^\infty \left\langle x^2(t) \right\rangle \exp\left(-\varepsilon t\right) d\, t \qquad x^2(t) = a^2 \sum_n n^2 \left|b_n(t)\right|^2$$

V.D.Lakhno, N.S.Fialko, *JETP Letters*, **78**, 336, (2003).

Temperature dependence of Hole mobility in (PolyG / PolyC)

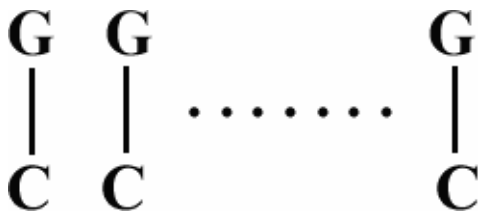

$\nu = 0{,}084\,\text{eV}, \quad \alpha' = 0{,}13\ \text{eV}/\mathring{\text{A}},$

$\omega = \sqrt{K/M} = 10^{12}\ \text{sec}^{-1}, \omega' = \gamma_f / M = 6 \cdot 10^{11}\text{sec}^{-1}$

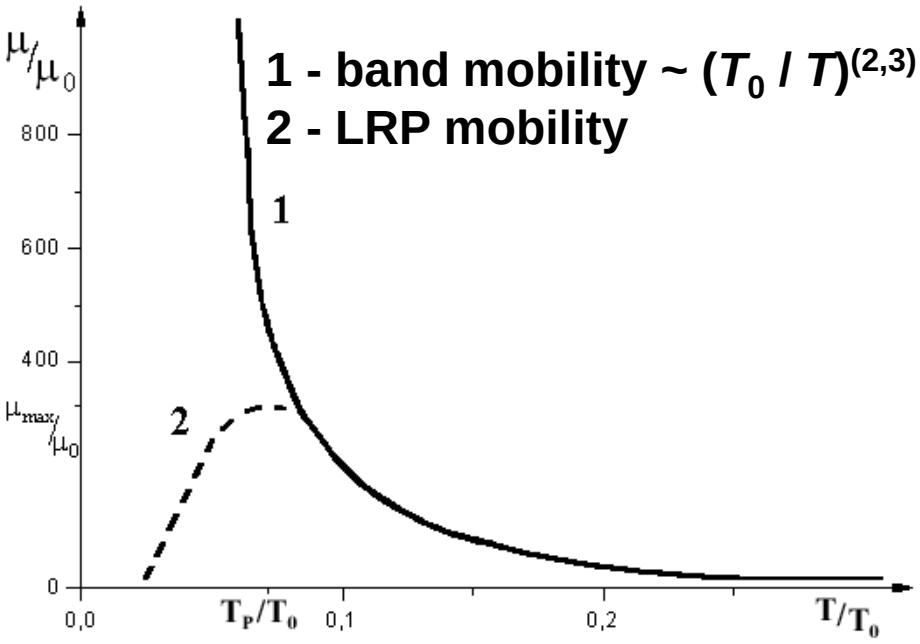

1 - band mobility ~ (T_0 / T)$^{(2,3)}$

2 - LRP mobility

$\hbar\omega \approx 7{,}7\,K, \quad T_P \approx 20\,K,$

$\mu_{\max} \approx 1500$ cm ^{2}/ V sec,

$\mu_0 = 2{,}87$cm ^{2}/ V sec -

hole mobility at T_0 = 300 K

Small radius polaron near critical temperature

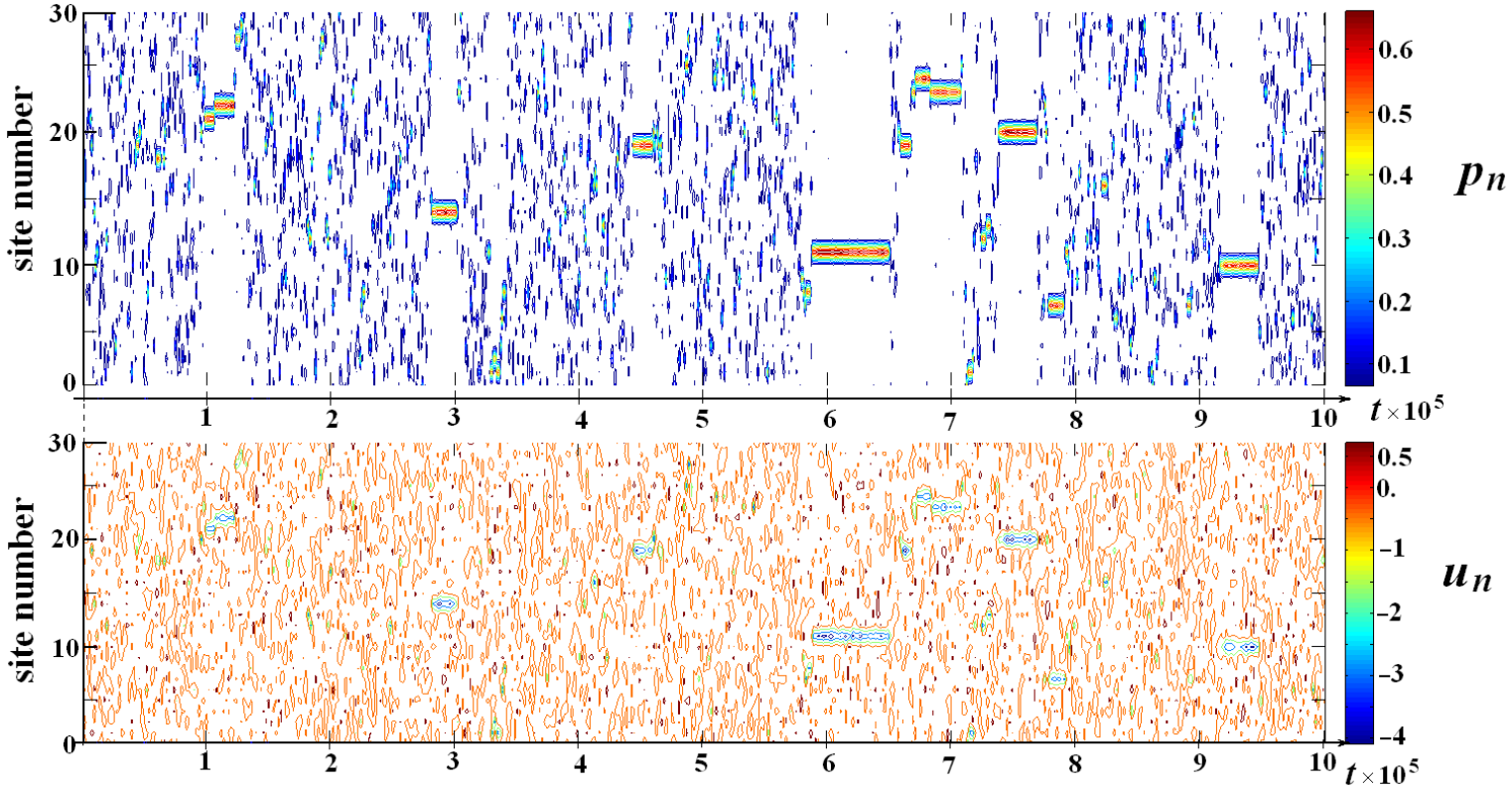

Localized and delocalized charge states

Delocalisation parameter

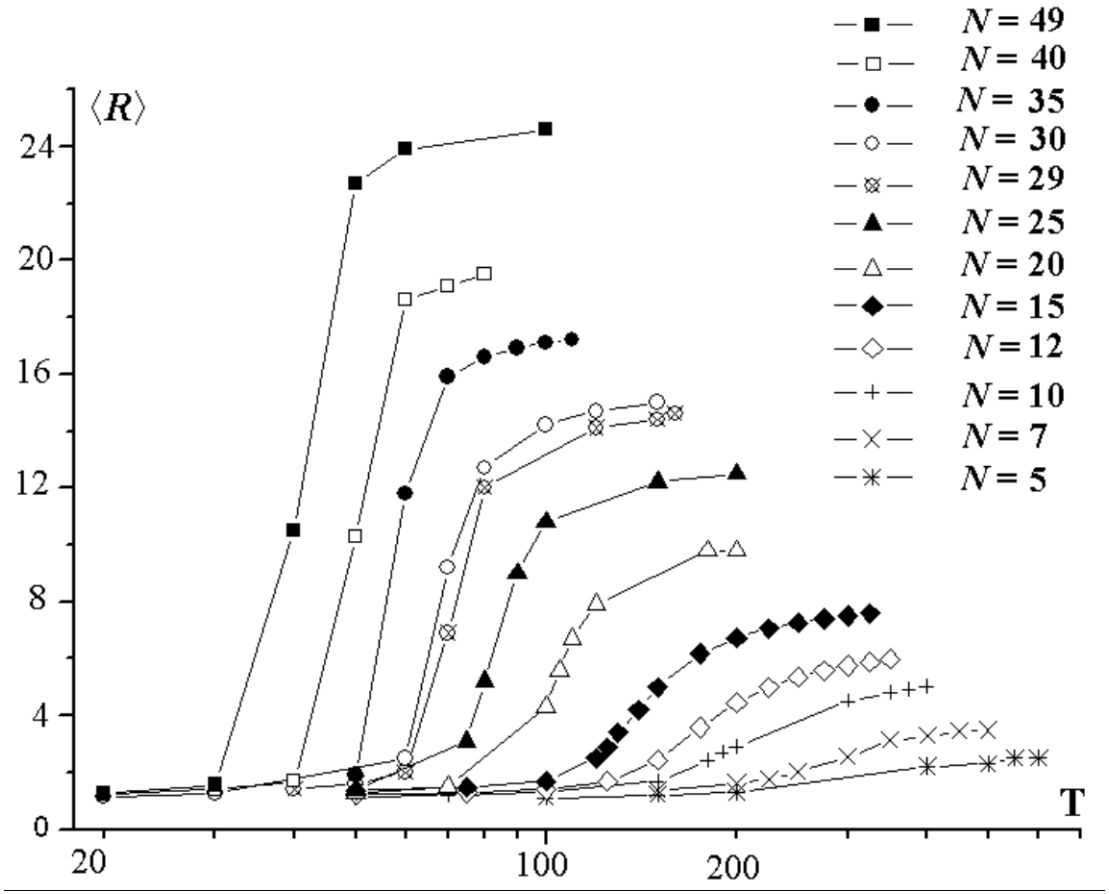

$$\langle R \rangle = \left\langle \frac{1}{\sum |b_n|^4} \right\rangle$$

$$\langle R \rangle = 1, \quad |b_n|^2 = \delta_{n,n_0};$$

$$\langle R \rangle = N, \quad |b_n|^2 = 1/N$$

Thermodynamic values of $\langle R(T) \rangle$ for chains of different lengths N (logarithmic scale).

V.Lakhno,N.Fialko, JETP, v.120,125,(2015)

Polaron energy

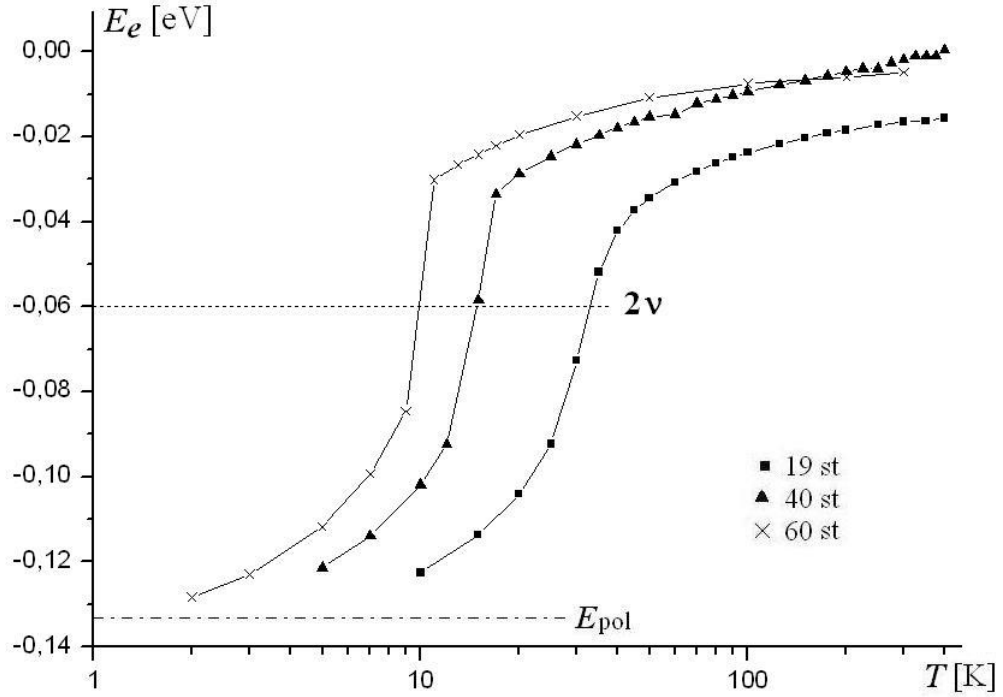

Results of calculations of thermodynamically equilibrium values.

Electronic part of the total energy Ee(T) for chains of length 19, 40 and 60 sites. Dashed lines show polaron energies Epol and the lower bound of the conductivity band 2ν

Heat capacity

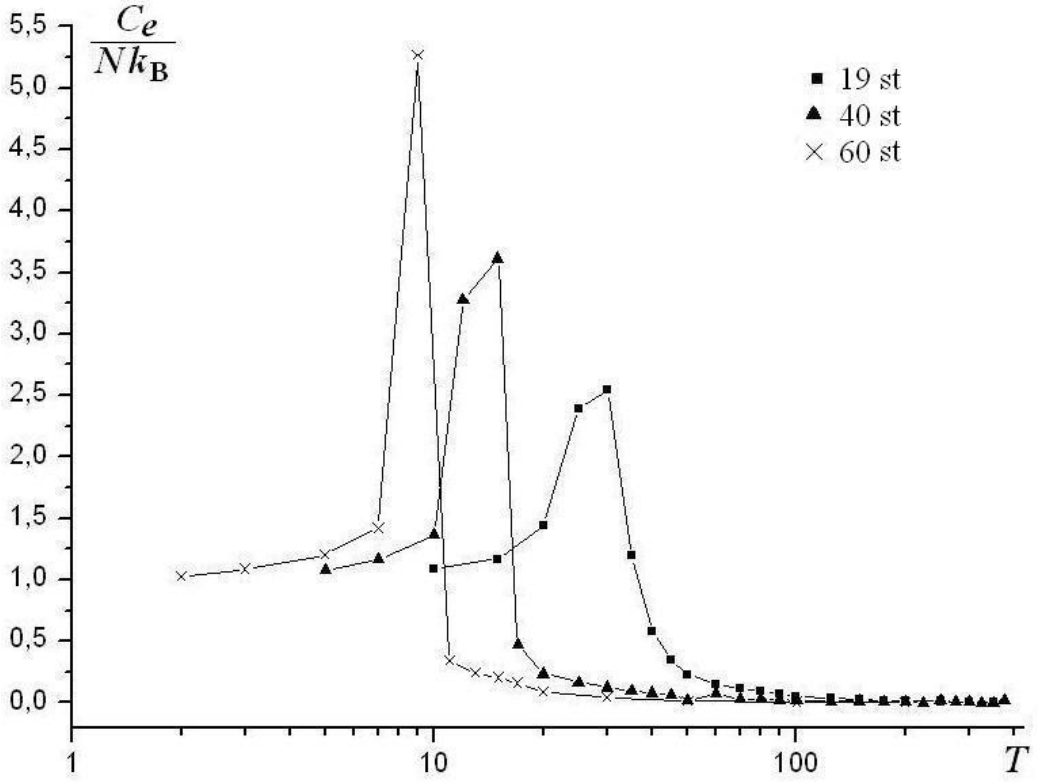

Normalized electronic heat capacity.

$$C_V = \frac{\partial \langle E_{tot}(T) \rangle}{\partial T} = \frac{1}{k_B T^2} \left(\langle E_{tot}^2(T) \rangle - \langle E_{tot}(T) \rangle^2 \right), \qquad C_e = \frac{\partial E_e}{\partial T} = C_V - Nk_B$$

Conclusion

1. For T=0, $E_e=E_{pol}$, temperature grows,$E_e(T)$ increases and f charge passes on from polaron state to delocalized one.
2. The polaron decay temperature depends not only on the model parameters but also on the chain length: the larger is N, the less is the decay temperature.
3. The peak on the graph of electronic heat capacity is observed at the polaron decay temperature.

DNA-based molecular devices

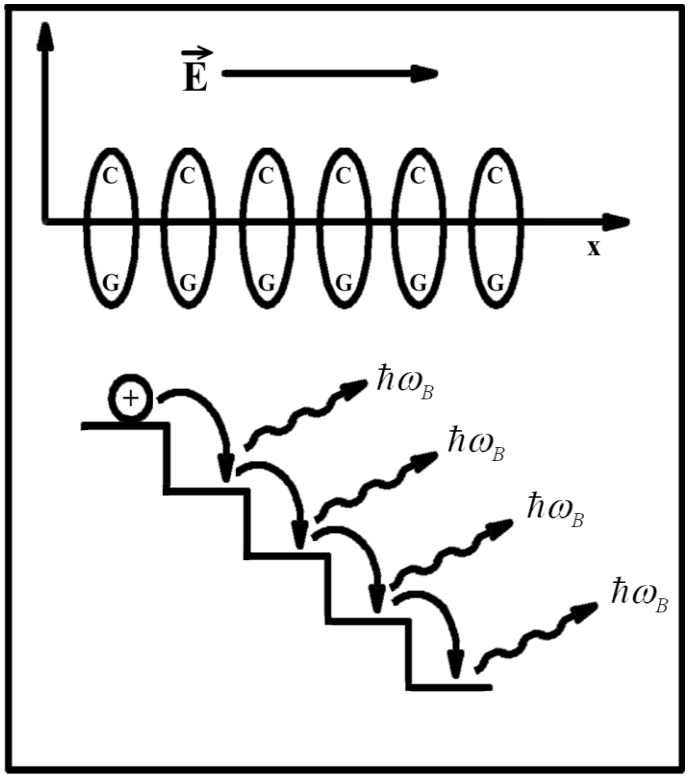

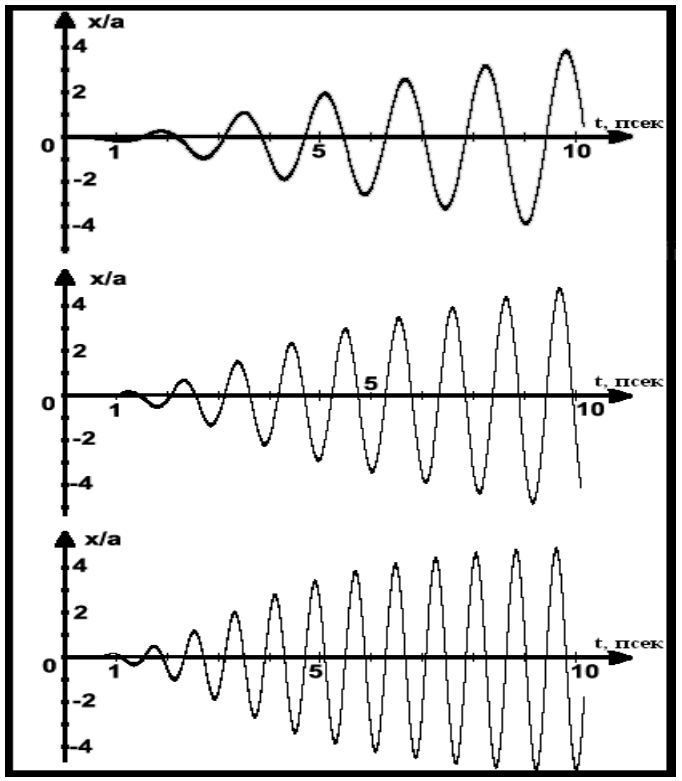

$$\hbar\Omega = n\hbar\omega_B,\ n = 1,2,3,\ldots\ \hbar\omega_B = eEa$$

- **Terahertz emitters of electromagnetic waves**
- **Nanoelements with negative differential conductivity**
- **Nanoelements with absolute negative conductivity**
- **Multiphoton radiation detectors**
- **Cascade lasers**

Continuous-wave two-photon terahertz quantum cascade laser

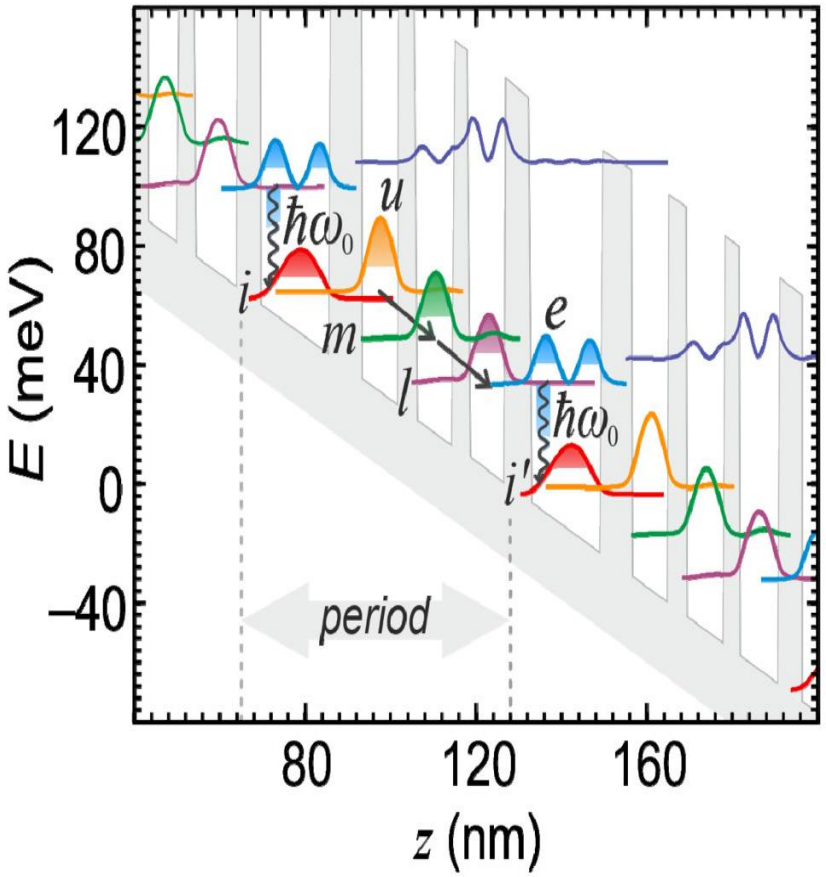

Conduction band diagram and squared moduli of electron wave functions, calculated by the k·p method, for the optimized structure of a THz QCL based on GaAs/Al0.15Ga0.85As at a temperature T = 70 K and a voltage across the structure period V = 66 mV. Arrows indicate radiative transitions. The dashed rectangle marks the period of the cascade structure.

J. Appl. Phys. 136, 194504 (2024); doi: 10.1063/5.0230491

Electronic nanopore sequencing

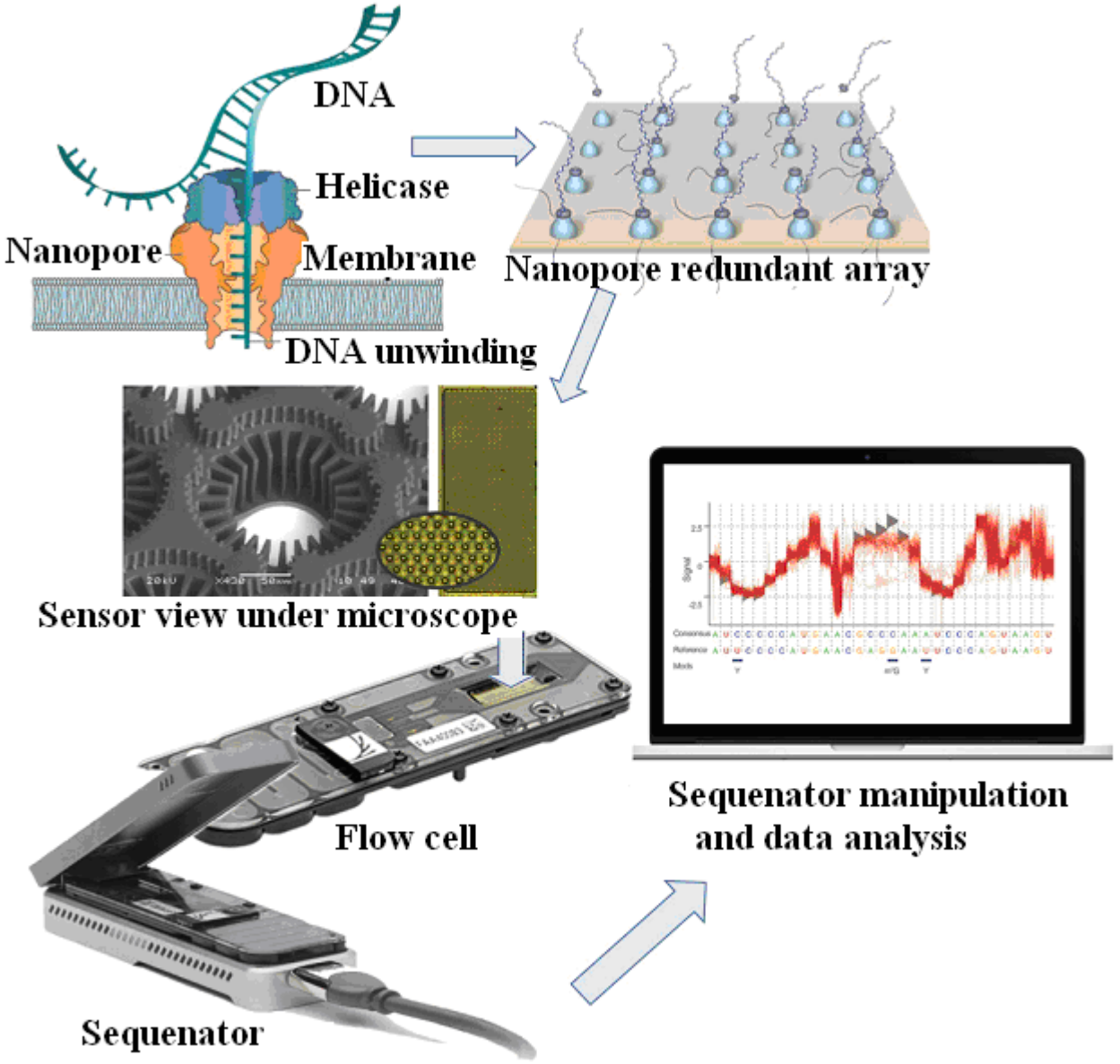

Nanobiochip

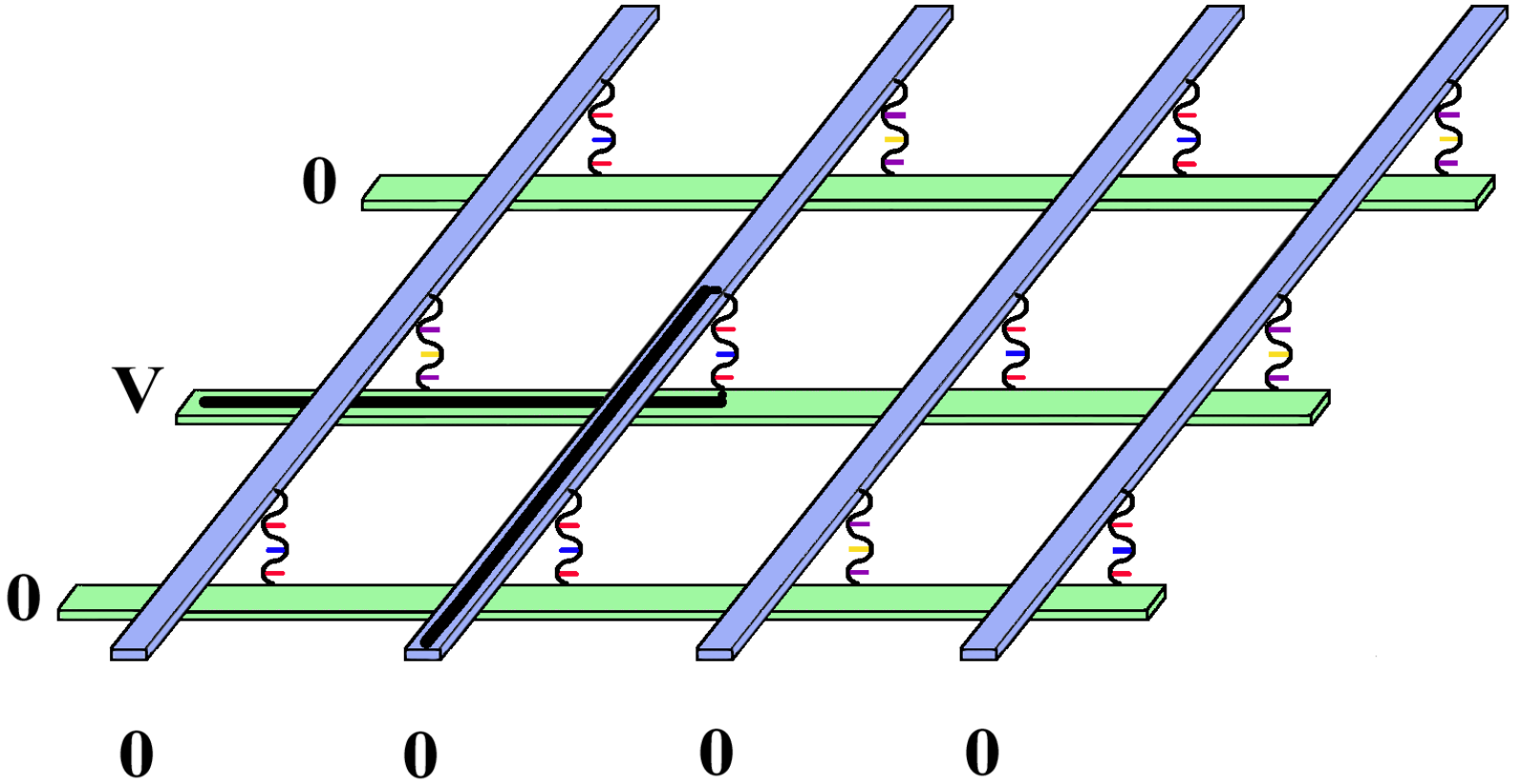

The measuring of current along the separated contour diagnoses its change after hybridization

V. D. Lakhno, V. B. Sultanov.
J. Chem. Theory Comput. **2007, 3, 703-705**

Digital memory device based on tobacco mosaic virus conjugated with nanoparticles

Nature v. 1 Oct. 2006, pp.72-77

R.J. Tseng[1], CH. Tsai[2], L. Ma[1], J. Ouyang[1], C.S. Ozkan[3] Y. Yang[1]

[1]Department of Materials Science and Engineering, University of California_Los Angeles, USA

[2]Department of Electrical Engineering, University of California_Riverside, USA

[3]Department of Mechanical Engineering, University of California_Riverside, USA

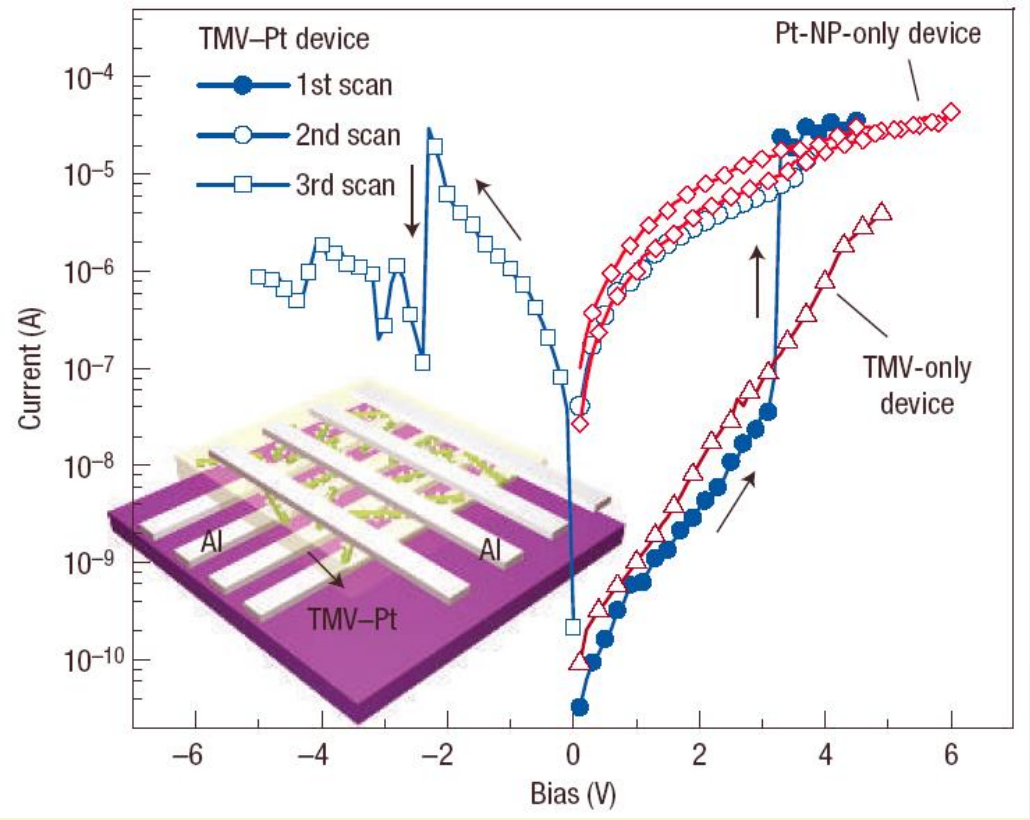

Logical gate XOR

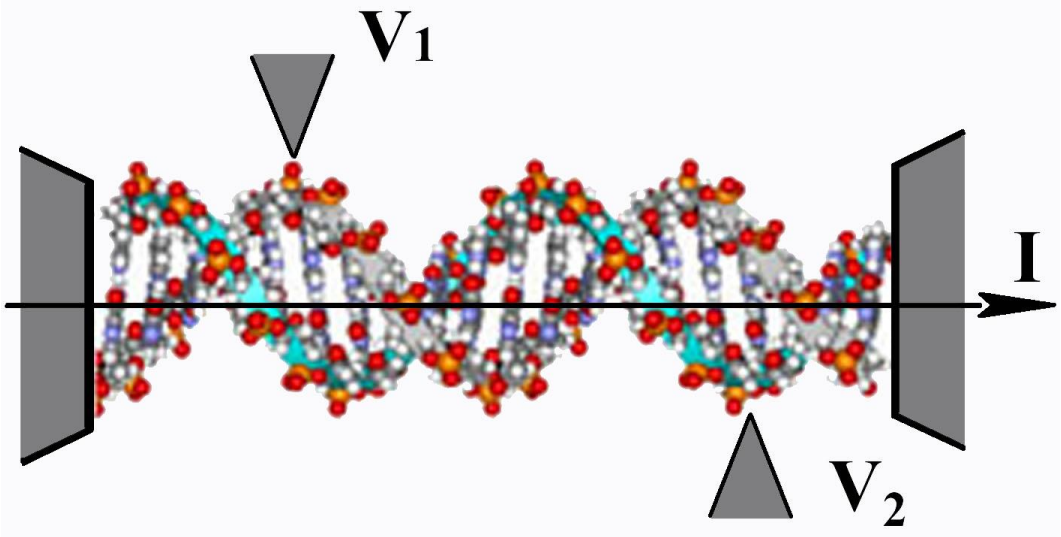

v1	v2	p
1	1	0*
1	0	1
0	1	1
0	0	0

V. D. Lakhno, V. B. Sultanov. Mathematical biology and bioinformatics, 2006, v.1 (1), pp. 123-126.

Quadruplexes: the future of nanobioelectronics and nanobioinformatics

1. Extremely small feature size (molecular or atomic scale)
2. Ultra-low power consumtion
3. Absence of dissipation
4. Absence of charge transfer
5. Developed circuitry
6. Ability to self-assemble

DNA quantum cell

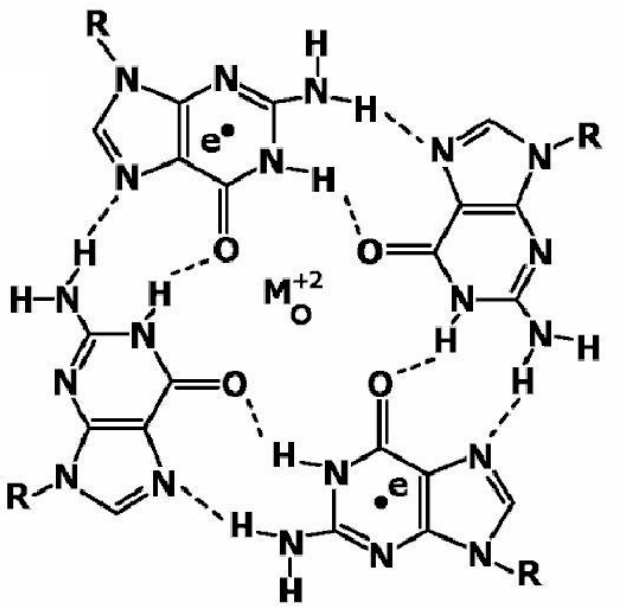

G-quadruplex

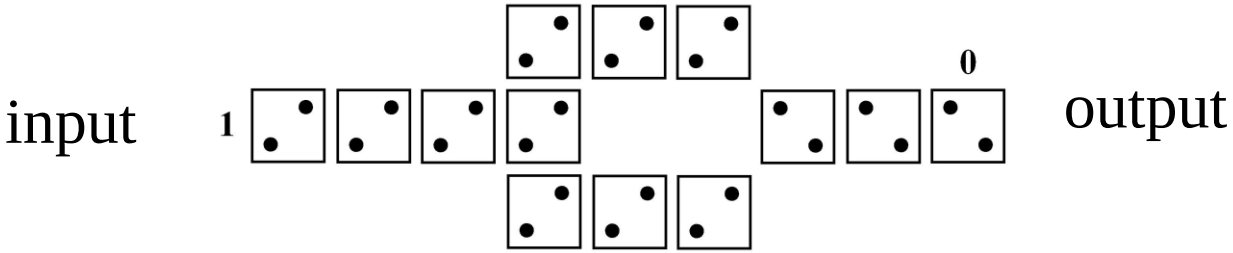

inverter

A.B.Kotlyar, D.Porath et al. Nature nanotechnology, 2014, pp. 1040-1046.

DOI: 10.1038/NNANO.204.246

Сейчас не удается отобразить рисунок.

Динамика квантового клеточного автомата на основе квадруплексов ДНК

Лахно В.Д.

Институт математических проблем биологии РАН – филиал ФИЦ Институт прикладной математики им. М.В. Келдыша РАН

lak@impb.ru

Квадруплекс ДНК на основе гуанинов, допированный двумя электронами (дырками), рассматривается как единичный кубит для выполнения квантовых вычислений. С использованием гамильтониана Хаббарда получены динамические уравнения для симуляции динамики квантового кубита на классическом компьютере.

Ключевые слова: квантовые вычисления, приближение ближайших соседей.

Dynamics of a Quantum Cellular Automaton Based on DNA Quadruplexes

Lakhno V.D.

Institute of Mathematical Problems of Biology – Branch of Keldysh Institute of Applied Mathematics, Russian Academy of Sciences

A guanine-based DNA quadruplex doped with two electrons (holes) is considered as a single qubit for performing quantum computations. Using the Hubbard Hamiltonian, dynamic equations are obtained to simulate the dynamics of a quantum qubit on a classical computer.

Key words: quantum calculations, nearest neighbor approximation.

1. Основной раздел

Хорошо известно, что квантовые клеточные автоматы (ККА) способны осуществлять квантовые вычисления. Идея использования для этой цели квадруплексов ДНК была впервые высказана автором в работе [1]. Изображённая на рис. 1а структура квадруплекса ДНК реализует схему квантового клеточного автомата (1б, 1в), в которой чёрными кружками отмечены возможные положения электронов (дырок) на гуанинах квадруплекса в поляризованных состояниях P1 и P2.

Для разработки симулятора квантовых вычислений на основе ККА важно уметь описывать динамику состояний P1 и P2. С этой целью используем гамильтониан ККА [2]:

$$\hat{H} = \sum_{i,\sigma} E_i \hat{n}_{i,\sigma} + \sum_{i>j,\sigma} \left(T_{ij}\hat{a}^{+}_{i,\sigma}\hat{a}_{j,\sigma} + T_{ji}\hat{a}^{+}_{j,\sigma}\hat{a}_{i,\sigma}\right) + \\ + \sum_i U\hat{n}_{i\downarrow}\hat{n}_{i\uparrow} + \sum_{i>j,\sigma,\sigma'} V_{ij}\hat{n}_{i,\sigma}\hat{n}_{j,\sigma'}, \qquad (1)$$

$$\hat{n}_{i,\sigma} = \hat{a}^{+}_{i\sigma}\hat{a}_{i,\sigma}.$$

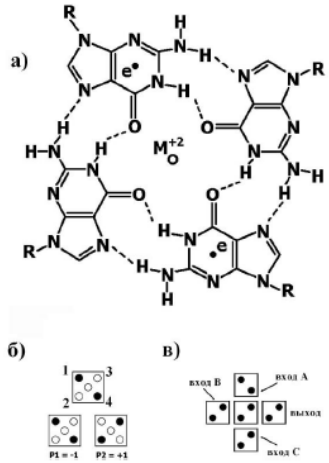

Рис. 1. Квантовые клеточные автоматы на основе гуаниновых квадруплексов.

Proceedings of the International Conference "Mathematical Biology and Bioinformatics". Ed. V.D. Lakhno.
Vol. 10. Pushchino: IMPB RAS, 2024. Paper No. e. doi: 10.17537/icmbb24.

В приближении ближайших соседей, $T_{i,j} = \eta$, если $i = j \pm 1$, $i = 1,2,3,4$ и равны нулю во всех других случаях, E_i – энергия электрона на каждом из гуанинов на рисунке 1,б, U – энергия кулоновского отталкивания, когда на одном гуанине находится два электрона; $\hat{a}_i^+, \hat{a}_i$ – операторы рождения и уничтожения электрона на каждом из гуанинов. Будем искать волновую функцию гамильтониана (1) $|\Psi\rangle$ в виде:

$$|\Psi\rangle = \sum_{ij} \Psi_{ij}(t)\hat{a}_i^+ \hat{a}_j^+ |0\rangle, \quad \sum_{ij}\left|\Psi_{ij}\right|^2 = 1 . \quad (2)$$

В (2) мы включили спиновые индексы σ_i в индекс i. С использованием (2) уравнение Шрёдингера для компонент Ψ_{ij} примет вид:

$$\eta(\Delta\Psi)_{ij} + U\delta_{ij}\Psi_{ij} + V_{ij}\Psi_{ij} + \left(E_i + E_j\right)\Psi_{ij} = \\ = \sqrt{-1}\dot{\Psi}_{ij}, \quad (3)$$

где $\left(\Delta\Psi_{ij}\right)$ = дискретный оператор Лапласа:

$$\left(\Delta\Psi_{ij}\right) = \Psi_{i-1,j} + \Psi_{i+1,j} + \Psi_{i,j-1} + \Psi_{i,j+1} \quad (4)$$

Отметим, что динамика заселённости i – го гуанина в квадруплексе P_i определяется выражением: $P_i(t) = \sum_j\left|\Psi_{ij}(t)\right|^2$. Таким образом состоянию P1 соответствует $P_{1,4} \approx 1, P_{2,3} \approx 0$, P2 соответствует $P_{2,3} \approx 1, P_{1,4} \approx 0$. Состояния P1 и P2 являются осциллирующими величинами и могут быть использованы для проведения квантовых вычислений.

Шестнадцать уравнений (3) и (4) моделируют динамику одного кубита. Схема из N клеточных автоматов (N – кубитов) содержит 16^N уравнений. По этой причине на классическом суперкомпьютере реально симулирование порядка десяти кубитов.

4. Список литературы

1. Lakhno V.D. DNA nanobioelectronics. *Int. J. Quant. Chem.* 2008. V. 108. P. 1970–1981.
2. Валиев К.А., Кокин А.А. *Квантовые компьютеры: надежды и реальность.* Москва-Ижевск. РХД 2001. С.

The results were obtained in collaboration with my colleagues:

N.Fialko

V.Sultanov

A.Korshunova

A.Shigaev

E.Sobolev

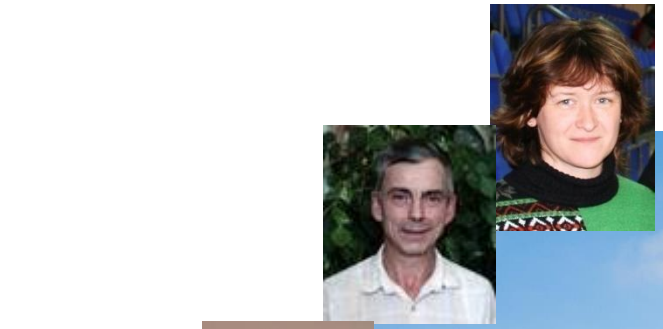

Thank you for your attention